TITLE PAGE

Title: IMAGING RESERVOIR QUALITY: SEISMIC SIGNATURES OF GEOLOGIC PROCESSES

Type of Report: Project Evaluation Report
Reporting Start Date: January 1, 2005
Reporting End Date: December 31, 2006
Principal Investigator: Prof. Gary Mavko
Date of Report: April 2007
DOE Award Number: DE-FC26-04NT15506
Submitting Organization: Stanford University, 651 Serra Street, Suite 220, Stanford, CA 94305-6203

DISCLAIMER

This report was prepared as an account of work sponsored by an agency of the United States Government. Neither the United States Government nor any agency thereof, nor any of their employees, makes any warrantee, express or implied, or assumes any legal liability or responsibility for the accuracy, completeness, or usefulness of any information, apparatus, product, or process disclosed, or represents that its use would not infringe privately owned rights. Reference herein to any specific commercial product, process, or service by trade name, trademark, manufacturer, or otherwise does not necessarily constitute or imply its endorsement, recommendation, or favoring by the United States Government or any agency thereof. The views and opinions of authors expressed herein do not necessarily state or reflect those of the United States Government or any agency thereof.

ABSTRACT

This first part of the study documents the similarity in the rock physics patterns of sand-rich deep-water deposits from offshore Gulf of Mexico and other similar depositional environments. Lithofacies successions from diverse depositional environments show distinctive patterns in various rock-physics planes (seismic velocity-porosity, velocity-density and porosity-clay volume). Four clear examples of decameter-scale lithofacies sequences are documented in this study: (1) fluvial deposits from the Miocene of Colombia show an inverted-V pattern indicative of mm- to cm-scale dispersed fabric in the mixed lithofacies, (2) a fining-upward lithofacies sequence of mud-rich deep water deposits from offshore West Africa shows a linear trend associated with mm- to cm-scale horizontally laminated sand-clay mixtures, (3) sand-rich deep water deposits from offshore Gulf of Mexico present a pattern resulting from the scarcity of mixed lithofacies, and (4) a coarsening-upward lithofacies sequence of shallow marine deposits from Colombia presents evidence of both dispersed and horizontally laminated mixed lithofacies, with predominating dispersed mixtures generated by bioturbation..

In the second part of this study, we illustrate a workflow for establishing improved links between sedimentary processes, as might be inferred from a sequence stratigraphy analysis, and seismic amplitudes. The strategy is to estimate plausible, though uncertain, rock properties, such as composition, grain size, sorting, and porosity from the geologic interpretation. These candidate rock properties are then used as inputs to rock physics models that predict the corresponding elastic properties that control seismic wave propagation. Comparison of the model predictions with observed seismic amplitudes allows us to get improved estimates of the reservoir properties. More complete field data sets have been received, on which the workflow will be applied in the project continuation.

The third part of this study presents an analysis of how packing and sorting variations impact rock elastic properties. It has previously been established that depositional variations often lead to a particular velocity-porosity relation that can be well described using a modified lower elastic bound. The current work illustrates how packing, the result of post-depositional processes, yields a similar trend. Both sorting and backing influence porosity, permeability, and their elastic signatures.

TABLE OF CONTENTS

TITLE PAGE 1

Title: Imaging Reservoir Quality: Seismic Signatures of Geologic Processes 1

DISCLAIMER 2

ABSTRACT 3

TABLE OF CONTENTS 4

LIST OF GRAPHICAL MATERIALS 5

EXECUTIVE SUMMARY 6

REPORT DETAILS 8

OBJECTIVE 8

APPROACH 8

RESULTS DURING BUDGET PERIOD 1 10

ACCOMPLISHMENTS DURING BUDGET PERIOD 1 11

RESULTS DURING BUDGET PERIOD 2 12

ACCOMPLISHMENTS DURING BUDGET PERIOD 2 20

REFERENCES 20

ABREVIATIONS AND ACRONYMS 23

PROJECT STATUS REPORT 24

MILESTONE LOG 26

ATTACHMENT A 27

ATTACHMENT B 37

LIST OF GRAPHICAL MATERIALS

Figure 1: Three parasequences (PS) interpreted within progradational depositional lobes. Changes in sorting is abrupt across the para-sequence boundaries and gradual along the boundaries.

Figure 2: In well log blocky motif corresponds to aggradational / channel deposits and coarsening-up motif corresponds to progradational depositional lobes.

Figure 3. Well-log data from two different lithofacies sequences: (a) fining-upward lithofacies sequence from fluvial deposits of the Miocene Guayabo Formation (Llanos Basin Colombia); (b) Figure 3: The scatter points show measurements of porosities and velcities from well log in prograding lobes. The magenta line is obtained using rock physics modeling for unconsolidated sand.

Figure 4: AVO modeling results: Intercept and Gradient crossplot color-coded by porosity. They indicate distinct trend of variation in reservoir properties from landward to basin-ward

Figure 5: The depositional trend of sands in the velocity-porosity plane. The data corresponds to uncemented sands from fluvial deposits (well Apiay-1). Data color-coded by clay fractio (Vclay).

Figure 6: Well-log data of sandstones from one single stratigraphic sequence within an oil field. The graph shows the three main trends for sandstones: the flat trend associated with the sorting effect, the compaction trend, and the steep diagenetic trend. As predicted from the theoretical model, the MHSLB constitutes an upper bound for the sorting trend.

EXECUTIVE SUMMARY

We report the results of our primary efforts completed during budget periods 1 and 2. During budget period 1, lithofacies successions from diverse depositional environments were studied to understand their distinctive patterns in various rock-physics planes (seismic velocity-porosity, velocity-density and porosity-clay volume). These patterns are the consequence of textural and compositional variations in the mm- to cm-scale fabric associated with the mechanics of deposition, and coeval post-depositional processes like bioturbation. Four clear examples of decameter-scale lithofacies sequences were documented in this study: (1) fluvial deposits from the Miocene of Colombia show an inverted-V pattern indicative of mm- to cm-scale dispersed fabric in the mixed lithofacies, (2) a fining-upward lithofacies sequence of mud-rich deep water deposits from offshore West Africa shows a linear trend associated with mm- to cm-scale horizontally laminated sand-clay mixtures, (3) sand-rich deep water deposits from offshore Gulf of Mexico present a pattern resulting from the scarcity of mixed lithofacies, and (4) a coarsening-upward lithofacies sequence of shallow marine deposits from Colombia presents evidence of both dispersed and horizontally laminated mixed lithofacies, with predominating dispersed mixtures generated by bioturbation. The applicability of the patterns observed to predict the seismic properties of larger sequences and away from well control depends on vertical and lateral persistence of the lithofacies assemblage.

In the second budget period, our efforts focused on two complementary studies. The first study formulates a workflow aimed at integrating the important constraints derived from sequence stratigraphy with rock physics models to reduce the uncertainty of seismic reservoir characterization. The second study focuses on understanding how parameters, grain packing and sorting, influence seismic velocity.

Sequence stratigraphy is the geologic interpretation of process/response events that can predict the likely occurrence of reservoir facies, source rocks and seals. Traditional stratigraphic interpretation from post-stack seismic data has been predominantly qualitative based on visual inspection of geometric patterns in the seismic reflections. However, quantitative interpretation of seismic amplitude is possible if we can extract information about compositional maturity (mineralogy, clay content) and textural maturity (sorting, grain angularity, sphericity and roundedness) using principles of sedimentology. We have preliminarily applied this concept in a deep-water turbidite system from Campos Basin, offshore Brazil. Our interpretation was based on (a) basin history (b) geometry and truncation patterns of reflectors and (c) stacking patterns of well

logs. We considered three para-sequences within the prograding depositional lobes and used sequence stratigraphic principles to predict relative trends of sorting, an important control on porosity. Corresponding elastic properties were estimated using the soft-sediment model, which combines Hertz-Mindlin contact mechanics with the Hashin-Shtrikman lower bound. AVO signatures at the sequence boundaries were predicted, showing, for example, distinct landward-basinward trends of intercept and gradient.

The soft sediment model trend is considered to be solely the effect of sorting. However, our mathematical models of demonstrate that packing also has an influence. The velocity-porosity trend observed in subsurface data agrees with the flat trend predicted from our theoretical analysis. A least-squares regression between sorting and porosity from the core data indicates a small negative correlation between porosity and the grain size, which indicates a minor influence of packing, probably associated with grain angularity (fine grains tend to be more angular than coarser sands). However, the effect of sorting on porosity, in these sands, is stronger than the effect of packing. The high-porosity have better sorting than the low-porosity clean sands. These two different types of sands create the flat trend observed in the velocity-porosity plane.

REPORT DETAILS

OBJECTIVE

The overall objective of this project is to improve the accuracy and resolution of interpreting lithofacies, pore fluids, and reservoir quality from seismic. A related goal is to establish quantitative rock physics links between highly successful, but often disconnected technologies, such as attributes analysis, AVO, seismic inversion (including acoustic and elastic impedance), 3D-seismic geomorphology, sequence and seismic stratigraphy, and basin modeling. Too often, quantitative seismic analysis, processing, and inversion are done without the benefit of geologic expertise, while geologic modeling and interpretation might be done without being able to quantify the seismic attributes that might distinguish multiple geologic hypotheses. A key to managing complexity and risk in exploration and production has always been effective integration of the diverse petroleum technologies. Workstations, visualization software, and geostatistics have contributed to integrating the vast amounts of *data* that we sometimes drown in. Perhaps more important are the asset teams that exploit diverse data by *integrating expertise.* Our objective includes helping to make the links between geology, seismic, and reservoir properties more *quantitative.*

APPROACH

Our approach is to introduce fundamental rock physics relations, which help to quantify the geophysical signatures of rock and fluid properties. Since rock properties are a consequence of geological processes, we begin to quantify the seismic signatures of various geologic trends. We also fully embrace probabilistic and geostatistical tools, as quantitative means for managing the inevitable uncertainty that accompanies all quantitative methods. Quantifying, managing, and understanding the uncertainties is critical for survival in a risky environment.

The results of this work will help to define an interpretation strategy for relating high-resolution seismic images of natural heterogeneities to the geologic systems and rock parameters that control the storage and mobility of natural hydrocarbons. Our approach is to combine, within the geologic framework of the basin and/or reservoir, carefully processed seismic, core-calibrated down-hole measurements, and engineering data to reliably characterize reservoir heterogeneities.

We are using a multidisciplinary approach to examine and quantify grain-scale processes in rocks and to explore how to quantitatively recognize those properties seismically. We will develop improved models for the elastic signatures of compaction and diagenesis not only for sands but also for shales and mixed lithologies. Geologic compaction trends are often described separately for sands and for shales. However, mixed lithologies pose interesting problems. Understanding these mixing laws can be critical to relating seismic signatures to sedimentary processes. The study will incorporate 3 main parts:

(1) **Geologic controls on rock microstructure.** We will work to better understand the variation of composition, fabric and physical properties of different types of shale according to their depositional environments, in order to distinguish them from sand reservoirs. From these, we will be using models and data to explore the impact of these fabrics on elastic properties.

(2) **Quantify the elastic (seismic) signatures** of lithology, textural maturity, pore pressure, and diagenetic processes of compaction, pressure solution, and cementation. We will evaluate the effect that stratigraphic sequences of different scales and their lithology trends have on seismic response.

(3) **Validate by integrating and interpreting reservoir field data.** We will combine the geologically calibrated rock physics relations with statistical analysis of the reservoir variability and measurement-related uncertainties. This will allow us to identify the most likely estimates of reservoir rock and fluid properties and their variation in space and time. Finally, we will quantify the uncertainties of these interpretations, and identify ways of reducing this uncertainty.

RESULTS DURING BUDGET PERIOD 1

Introduction

Our efforts during the budget period 1 were on Task 1 (Geologic controls on microstructure) and Task 2 (Quantifying elastic signatures).

Besides fluids and pressure, rock texture and lithofacies strongly influence seismic rock properties. The lateral variations in elastic properties of an intact, water-saturated, sedimentary rock, under uniform effective pressure and temperature, are determined by the lateral variations in clay content, sorting, packing, mineral composition, and cementation. These textural variations are the result of depositional and diagenetic processes. The impact of textural variations in seismic properties constitutes an important source of uncertainty in the prediction of reservoir properties from seismic data. Understanding the relationships between rock texture, fabric, and seismic response can reduce, or at least assess, the uncertainty associated with these predictions.

Methodology

This work involved the evaluation of well-log data from different basins and depositional environments.

We use three main cross plots to perform the analysis and comparison of the variation of elastic and bulk properties (porosity) within clastic depositional sequences: (1) bivariate histograms and color-coded cross plots of seismic P-wave velocity (Vp) and porosity (ϕ); (2) cross plots of porosity as a function of clay fraction (Vclay); and (3) color-coded cross plots of P-wave velocity and density. In general, we refer to these cross plots as the rock-physics planes.

The rationale behind this approach is the application of rock-physics diagnostics (Dvorkin and Nur, 1996) constrained to stratigraphic sequences (Gutierrez, 2001). We analyze the patterns of lithofacies sequences with a clear trend in clay content, inferred from both the gamma ray readings and the difference between neutron (NPHI) and density (PHID) porosities. In the cross plots the porosity corresponds to density porosity (PHID). The analyzed sequences correspond to genetically related lithofacies assemblages that form part of larger stratigraphic sequences.

Fluid substitution has been applied to velocity and density data in the case of hydrocarbon-bearing sands, in order to remove the fluid effect on the rock's elastic properties. Since the rocks analyzed are at similar pressure and temperature conditions, share a similar burial history, and have similar fluid saturations after fluid substitution, texture and composition are the dominant factors controlling the observed variations in elastic properties and porosity within any analyzed lithofacies sequence.

Rock-Physics Patterns of Selected Depositional Sequences

Four selected lithofacies sequences from different depositional environments, were studied to better understand the similarities and differences in their patterns of rock properties. The four sequences studied were: fluvial deposits of the Miocene Guayabo Formation from the Llanos Basin (Colombia), Miocene, mud-rich, deep-water deposits from offshore West Africa, sand-rich deep-water deposits from offshore Gulf of Mexico., and a coarsening-upward trend of shallow marine deposits from the Miocene Leon Formation, in the Llanos Basin (Colombia).

The fluvial deposits present a clear inverted-V pattern in the velocity-density plane, similar to the one predicted by the Marion-Yin model (Marion *et al.*, 1992). In the case of the mud-rich deep-water deposits, patterns are consistent with horizontally laminated sand-clay mixtures from the Backus average (e.g. Mavko et al, 1998), and the linear variation in porosity as a function of clay content. In contrast, the sand-rich deepwater deposits illustrate an absence of mixed lithofacies. Finally, there is a predominance of dispersed sand-clay mixtures in the shallow marine deposits, suggesting the occurrence of some subordinate laminated lithofacies.

The most striking difference occurs between the pattern outlined by the lithofacies sequence from fluvial deposits, and the pattern depicted by the lithofacies sequence from mud-rich deep-water deposits. The variations in clay content, density, porosity, and elastic properties observed in the fluvial deposits clearly indicate the predominance of a dispersed fabric in the mixed lithofacies. In contrast, the variations in clay content, density, porosity and elastic properties observed in the mud-rich deep-water deposits clearly indicate the presence of horizontally laminated sand-clay mixtures. Another significant difference is the contrast between the scarcity of mixed sand-clay lithofacies in the sand-rich deep-water deposits, and the abundance of both dispersed and laminar mixed lithofacies in the shallow marine deposits.

ACCOMPLISHMENTS DURNG BUDGET PERIOD 1

During this reporting period, we made significant progress in documenting and understanding how rock microtexture, and hence rock elastic properties, vary from location to location, while being controlled in a somewhat predictable way by sedimentologic processes. The results presented for this period of the project show that the existing rock-physics models predict the variations in elastic and hydraulic properties associated with the textural trends in clastic depositional sequences. The models, based on laboratory and theoretical analysis, can reproduce the patterns of clastic depositional

sequences in the rock-physics planes, based on well-log measurements. Mineral composition, sorting and the type of mixture are the main depositional lithofacies influencing the observed patterns. Cementation, compaction, pressure solution, and confining pressure are the dominant factors influencing the variations associated with diagenesis.

The variations observed among depositional sequences from diverse environments result from the intrinsic relationship that exists between textural trends, or lithofacies successions, and the flow regimes and conditions of sedimentation for each particular setting. These variations are produced by the presence, or absence, of mixed lithofacies and their specific fabrics. In general, ignoring the effect of mixed lithofacies and assuming that seismic reflections come from simple sand and shale interfaces can lead to erroneous interpretations.

RESULTS DURING BUDGET PERIOD 2

Introduction

We report the results of two primary efforts completed during the reporting period. The first study formulates a workflow aimed at integrating the important constraints derived from sequence stratigraphy with rock physics models to reduce the uncertainty of seismic reservoir characterization. The second study focuses on understanding how parameters, grain packing and sorting, influence seismic velocity. The key results of these efforts are highlighted in this report, and the technical details are given in the two attachments.

Reservoir Quality Prediction by Integrating Sequence Stratigraphy and Rock Physics.

Sequence stratigraphy is the geologic interpretation of process/response events (Mulholland, 1998). This can predict the likely occurrence of reservoir facies, source rocks and seals. Traditional stratigraphic interpretation from post-stack seismic data has been predominantly qualitative based on visual inspection of geometric patterns in the seismic reflections. However, quantitative interpretation of seismic amplitude is possible if we can extract information about compositional maturity (mineralogy, clay content) and textural maturity (sorting, grain angularity, sphericity and roundedness) using principles of sedimentology.

Quantitative seismic interpretation (Avseth et al., 2005) uses rock physics to link seismic amplitude with reservoir properties, like, porosity, clay-content, sorting, diagenetic cements etc. that are estimated from the stratigraphic analysis.

Our workflow consists of the following steps:

Step-1A: Understanding the systematic change of sedimentological properties with depositional cycles in a predictable fashion

VanWagoner et al. (1990) showed that the following sedimentological properties change predictably during transgression and regression:

- Sand-shale ratio
- Bed Thickness
- Grain-size
- Sorting
- Bio-turbation

Interestingly the changes in these sediment properties have opposite trends for transgression (shore line is approaching towards land) vs. regression (shore line is retreating towards basin). However there is uncertainty in these trends. During regression depositional energy tend to increase upward resulting in increase in bed-thickness, higher net-to-gross, better sorting and decrease in bio-turbation. On the other hand, marine transgression signifies decrease in depositional energy and exhibits an opposite trend of the above sediment parameters. These sediment parameters can be grouped as, compositional maturity and textural maturity parameters. They constitute important sediment properties that affect the elastic properties of the rocks and in turn affect seismic amplitudes.

Step-1B: Understanding spatial gradients of sedimentological properties

Gradients of sediment parameters are not same across the seismic reflector vs. along the reflector. Most seismic reflectors and their amplitude correspond to chronostratigraphic surfaces with a few exceptions. Chronostratigraphic surfaces represent depositional hiatus. Changes in sedimentological properties are abrupt across the hiatus and gradual along the hiatus (Emery and Myers, 1996).

The spatial gradients can be calibrated from well data. Estimating the lateral trends require multiple wells or horizontal wells. In the absence of such data one might assume that sediment parameters change linearly along the seismic reflector and in discrete steps

across the reflector. Thus, using sequence stratigraphy, we obtain relative trends of variation in sediment properties within a depositional sequence. These trends then constrain the input parameters in rock physics modeling.

Step-2: Rock physics analysis

Rock physics establishes the relation between sedimentological properties and elastic moduli. After we determine the spatial trends of sediment parameters in a stratigraphic package, appropriate rock physics models are selected. The input parameters are guided by our results from step 1. The rock models are calibrated to well log data. As output we obtain effective bulk modulus, shear modulus and density, as well as Vp and Vs as a function of porosity.

Step-3: AVO modeling and interpreting seismic amplitude

AVO forward modeling (Shuey's approximation) is used to obtain intercept and gradient at key stratigraphic interfaces using effective moduli predicted from rock physics analysis in step 2. Trends in compositional and textural maturity are carried through from sequence stratigraphy, to the AVO plane, via rock physics. Finally, the modeling results can be used to interpret observed amplitudes in terms of sedimentological properties and reservoir quality.

We have preliminarily applied this concept in a deep-water turbidite system from Campos Basin, offshore Brazil. Our interpretation was based on (a) basin history (Peres, 1990) (b) geometry and truncation patterns of reflectors (Figure 1) and (c) stacking patterns of well logs (Figure 2).

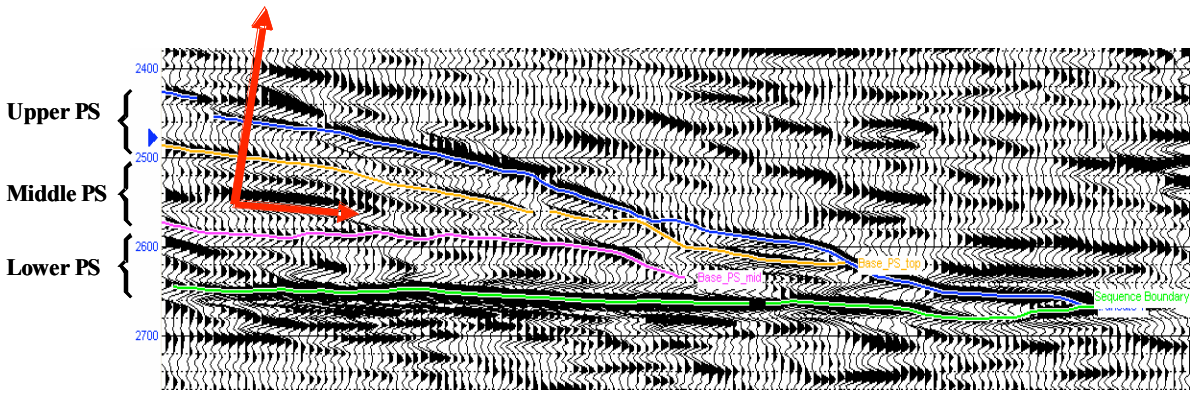

Figure 1: Three parasequences (PS) interpreted within progradational depositional lobes. Changes in sorting is abrupt across the para-sequence boundaries and gradual along the boundaries.

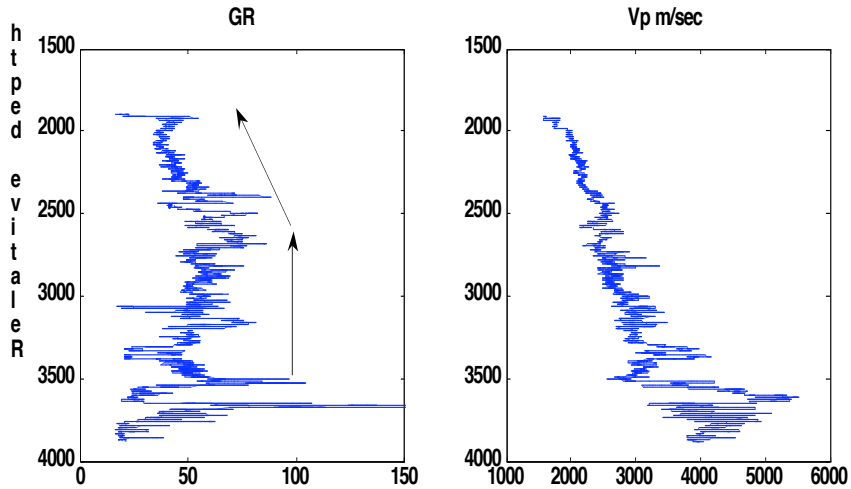

Figure 2: In well log blocky motif corresponds to aggradational / channel deposits and coarsening-up motif corresponds to progradational depositional lobes.

We considered three para-sequences (PS) within the prograding depositional lobes (Figure 1) and used sequence stratigraphic principles to predict relative trends of sorting, an important parameter that controls porosity, elastic moduli, and hence seismic velocities. We combined these trends with experimental sorting-porosity relationships for artificially mixed sand (Beard and Weyl, 1973; Jorden and Campbell, 1984).

To estimate elastic properties of the sediments, we used the soft sediment model (Dvorkin and Nur, 1996; Mavko et al., 1998) with a composition appropriate for compositionally mature sediments. Sediment elastic properies at zero porosity are simply the properties of the solid minerals; the sediment elastic moduli at critical porosity (~40%) are estimated using the Hertz-Mindlin theory for a packing of clean, well-sorted sphereical grains. Moduli of poorly sorted sand with porosities between 0 to critical porosity are interpolated between mineral point and well-sorted end member using the lower Hashin-Shtrikman bound. Figure 3 shows porosities and velocities obtained from a neighboring well log and the predicted velocities using the soft sediment model. Calibration of the model with well data is important for understanding the effects of mineralogy, effective stress, pore fluids, and porosity.

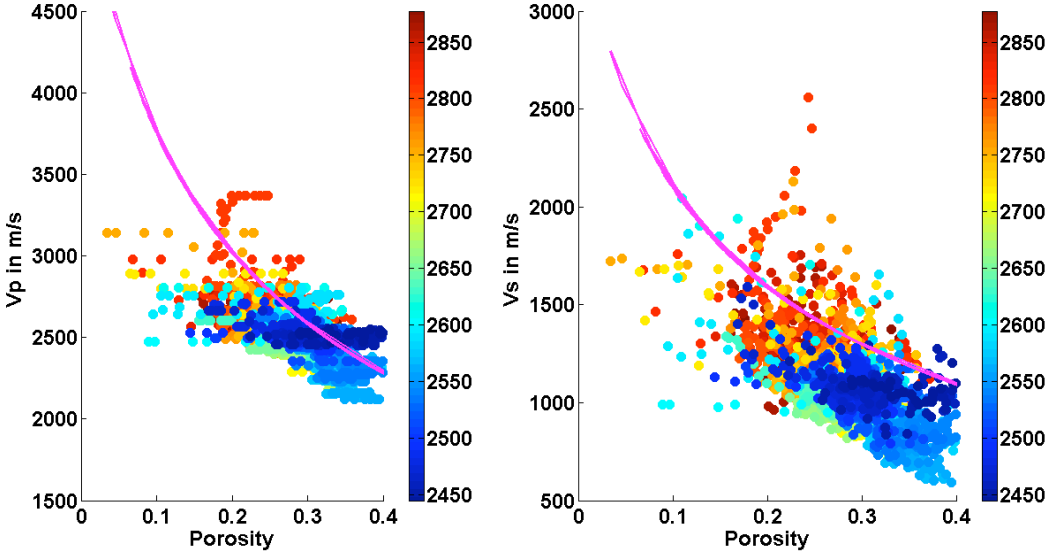

Figure 3: The scatter points show measurements of porosities and velcities from well log in prograding lobes. The magenta line is obtained using rock physics modeling for unconsolidated sand.

The corresponding effective Vp, Vs, and density are used to compute intercept (R0) and gradient (G) at the interfaces of the three para-sequences. They indicate distinct trends in R0-G plane (Figure 4). These trends can be used as a template to guide the interpretation of observed intercept and gradient from real seismic data

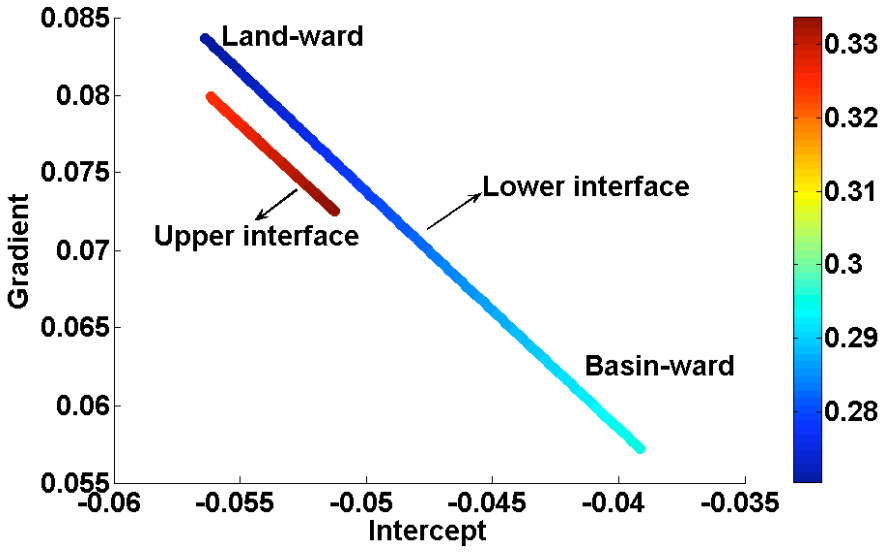

Figure 4: AVO modeling results: Intercept and Gradient crossplot color-coded by porosity. They indicate distinct trend of variation in reservoir properties from landward to basin-ward.

During the next year of this project, this preliminary workflow will be applied in more detail to data sets from offshore Africa and the North Sea.

Sorting and Packing Effects on the Elastic Properties of Sands

Sandstones at similar depths or confining pressures present a relatively flat trend in the velocity-porosity plane (Figure 5). This flat trend results from significant changes in porosity associated with very small changes in elastic stiffness. The main porosity-reduction mechanisms related to this flat-trend are matrix (clay) content, sorting, and mechanical compaction, as shown by Marion *et al.* (1992), Avseth *et al.* (2000), Dvorkin and Gutierrez (2001), Zimmer *et al.* (2002), and Zimmer (2003). For uncemented sandstones at the same pressure conditions, sorting and clay are considered to be the dominant mechanisms affecting this velocity-porosity trend. The trend can be reproduced using the modified Hashin-Shtrikman lower mound (MHSLB), and has been called the uncemented sandstone model (Mavko *et al.*, 1998), or the rock physics depositional trend (Avseth, 2000).

In the case of clean sand aggregates at similar pressure conditions, the uncemented trend is considered to be solely the effect of sorting (Avseth, 2000; Gutierrez, 2001). However, our mathematical models of identical spheres demonstrate that a similar effect can be obtained by changing the packing of the aggregate, without increasing the confining pressure. Therefore, packing and sorting seem to have a similar effect on the velocity-porosity trend.

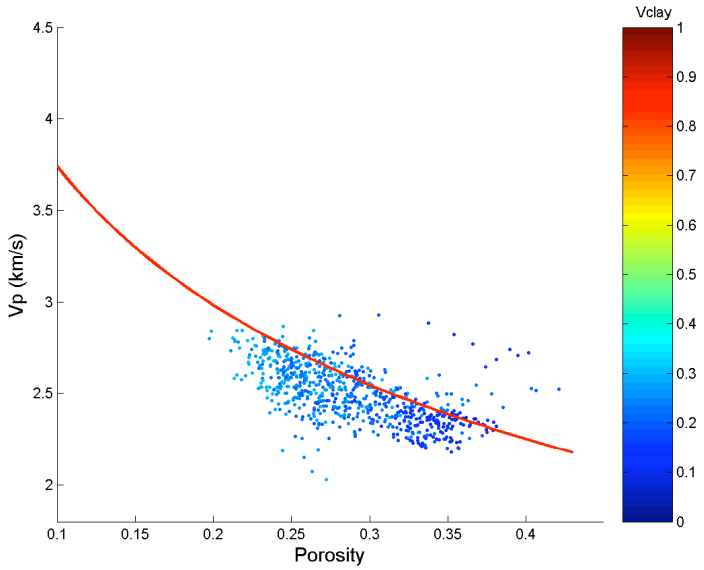

Figure 5: The depositional trend of sands in the velocity-porosity plane. The data corresponds to uncemented sands from fluvial deposits (well Apiay-1). Data color-coded by clay fractio (Vclay).

Given a similar stage of packing, porosity of granular materials decreases as the standard deviation of the grain-size distribution increases. In other words, porosity decreases as sorting deteriorates. This relationship has been demonstrated by various authors (Walton and White, 1937; Sohn and Moreland, 1968; Beard and Weyl 1973; and Zimmer, 2003).

Among several measures of packing the most common are the grain concentration, the coordination number (Allen, 2001), and the intergranular contact (Fuchtbauer, 1974). The grain concentration, or fractional volume concentration of particles (X), is directly related to porosity (ϕ):

$$\phi = 1 - X$$

The coordination number (C), the average number of grains in contact with each individual grain, affects the stiffness of the aggregate. The intergranular contact describes the type of grain contact –punctual, tangential, concave-convex, or sutured, and is usually a measure of the degree of mechanical compaction and pressure-solution, two processes related to diagenesis rather than to the depositional environment.

Like sorting, packing has a strong effect on porosity and therefore on permeability. The relationship between packing, coordination number and porosity has been analyzed by several authors (Graton and Fraser, 1935; Bourbie *et al*., 1987; Murphy, 1982; Cumberland and Crawford, 1987). The effect of packing on both porosity and permeability was extensively analyzed by Graton and Fraser (1935).

In order to take into account the effect of grain-size distributions on the effective elastic properties of granular material, our approach is to take the existing effective-medium models for uniform sphere packs, and modify them to incorporate the appropriate grain-size average. In other words, by finding the relevant averages of the variables involved in the computation, we can find approximate solutions to the effective elastic modulus.

In the case of idealized spheres, the main effects of grain rearrangement are reducing porosity and incrementing coordination number. Other possible additional effects involve grain stabilization and change in the grain-contact area.

There is good agreement between the sorting effect in both velocity and porosity observed in laboratory experiments (Zimmer, 2003), and the one predicted from our model presented in Attachment B.

The velocity-porosity trend observed in uncemented sandstones in the subsurface agrees with the flat trend predicted from our theoretical analysis (Figure 6). The flat trend is depicted by the shallower sands (blue dots in Figure 6), and follows a gentler slope than the one predicted from the unconsolidated sediment model (magenta lines in Figure 6). The velocity and porosity data shown correspond to well-log measurements obtained along an interval where core porosity and sorting data were also available. A least-squares regression was obtained for the correspondence between sorting and porosity from the core data. The least-squares regression also indicates a small negative correlation between porosity and the grain size, which indicates a minor influence of packing, probably associated with grain angularity (fine grains tend to be more angular than coarser sands). However, the effect of sorting on porosity, in these sands, is stronger than the effect of packing. The high-porosity have better sorting than the low-porosity clean sands. These two different types of sands create the flat trend observed in the velocity-porosity plane.

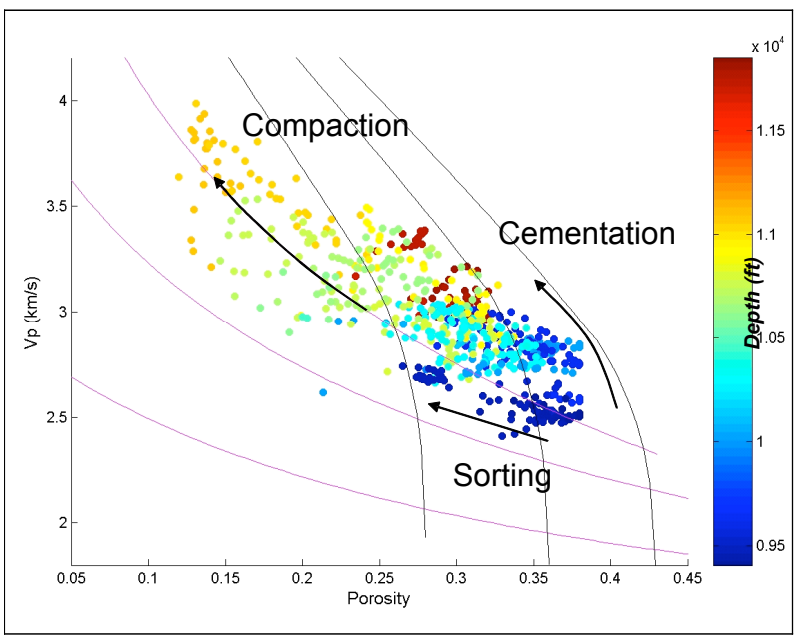

Figure 6: Well-log data of sandstones from one single stratigraphic sequence within an oil field. The graph shows the three main trends for sandstones: the flat trend associated with the sorting effect, the compaction trend, and the steep diagenetic trend. As predicted from the theoretical model, the MHSLB constitutes an upper bound for the sorting trend.

The theoretical analysis presented in this work indicates that the effect of sorting on both porosity and the elastic properties of granular materials differs from the effect of packing. This conclusion is also corroborated by the laboratory measurements and subsurface data. According to these results, variations in sorting generate a flatter trend in

the velocity-porosity plane, with a slope gentler than the modified Hashin-Shtrikman lower bound (MHSLB). In contrast, variations in packing tend to generate a steeper slope than that predicted using the MHSLB. In general, whereas the MHSLB is a reasonable upper bound for the sorting effect, it constitutes a lower bound for the packing effect.

ACCOMPLISHMENTS DURING BUDGET PERIOD 2

Two elements of this project have reported – theoretical modeling of the fundamental causes of elastic response to microstructure, and a workflow for applying these models for quantitative interpretation of seismic. The refined rock models, though never perfect, have shown excellent predictive power when compared with laboratory and field data. The workflow for applying these models involves a number of detailed steps, beginning with a careful stratigraphic interpretation of the seismic and log data. The workflow will be applied during the coming year on one or more high quality data sets that should provide for validation and refinement.

REFERENCES

Allen, J. R. L., 2001, Principles of Physical Sedimentology, George Allen & Unwin (Publishers), London, 272 p.

Avseth, P., J. Dvorkin, G. Mavko, and J. Rykkje, 2000, Rock physics diagnostic of North Sea sands: Link between microstructure and seismic properties. Geophysical Research Letters, 27, 2671-2764.

Avseth, P., Mukerji, T., and Mavko, G., 2005, Quantitative Seismic Interpretation: Applying Rock Physics Tools to Reduce Interpretation Risk: Cambridge University Press.

Avseth, P., 2000, Combining Rock Physics and Sedimentology for Seismic Reservoir Characterization in North Sea Turbidite Systems. Ph.D. thesis, Stanford University.

Beard, D. C., and P. K. Weyl, 1973, Influence of texture on porosity and permeability of unconsolidated sand. American Association of Petroleum Geologists Bulletin, 15, 2, 349-369.

Bourbie, T., O. Coussy, and B. Zinsner, 1987, Acoustics of Porous Media, Gulf Publishing Co., Houston, 334 pp.

Cumberland, D. J. and R. J. Crawford, 1987, The Packing of Particles, Elsevier Science Publishers, Amsterdam.

Dvorkin, J., and M. A. Gutierrez, 2001, Textural sorting effect on elastic velocities, part II: elasticity of a bimodal grain mixture, Society of Exploration Geophysicist Annual Meeting, Expanded Abstracts.

Dvorkin, J., and Nur, A., 1996, Elasticity of high-porosity sandstones: Theory for two North Sea datasets: Geophysics, 61, 1363-1370.

Emery, D., and Myers, K., 1996, Sequence stratigraphy: Blackwell scientific publications, Inc.

Fuchtbauer, H., 1974, Sediments and Sedimentary Rocks 1, in Sedimentary Petrology by W. v. Engelhardt, H. Fuchtbauer and G. Muller, Part II. John Wiley and Sons, New York, 464 pp.

Graton, L. C., and H. J. Fraser, 1935, Systematic packing of spheres –with particular relation to porosity and permeability: Journal of Geology, 43, 785-909.

Gutierrez, M., 2001, Rock physics and 3D Seismic Characterization of Reservoir Heterogeneities to Improve Recovery Efficiency, Ph. D. dissertation, Stanford University.

Jorden, J. R., and Campbell, F. L., 1984, Well Logging I - rock properties, borehole environment, mud and temperature logging: Society of Petroleum Engineers (SPE) of American Institute of Mining, Metallurgical and Petroleum Engineers (AIME).

Marion, D., A. Nur, H. Yin, and D. Han, 1992, Compressional velocity and porosity in sand-clay mixtures, Geophysics, 57, 4, 554-563.

Mavko, G., J. Dvorkin, and T. Mukerji, 1998, The Rock Physics Handbook, tools for seismic analysis in porous media, Cambridge University press, New York, pp 329.

Mulholland, J.W., 1998, Sequence stratigraphy: basic elements, concepts and terminology: The Leading Edge, 17, 37-40.

Murphy, D. W., III, 1982, Effect of Microstructure and Pore Fluids on The Acoustic Properties of Granular Sedimentary Materials, Ph. D. dissertation, Stanford University.

Peres, W.E., 1990, Seismic-stratigraphic study of the Oligocene-Miocene shelf-fed turbidite systems of the Campos Basin, Brazil: Ph.D. thesis, The University of Texas at Austin.

Sohn, H. Y. and C. Moreland, 1968, The effect of particle size distribution on packing density, Canadian Journal of Chemical Engineering, 46, 162-167.

Van Wagoner, J.C. ., Mitchum, R.M., Campion, K.M., and Rahmanian, V.D., 1990, Siliciclastic sequence stratigraphy in well logs, cores and outcrops: The American Association of Petroleum Geologists, Methods in Exploration Series, no. 7.

White, H. E., and S. F. Walton, 1937, Particle packing and particle shape, Journal of the American Ceramists Society, 20, 155-166.

Zimmer, M., M. Prasad, and G. Mavko, 2002, Empirical velocity-pressure and porosity-pressure trends in unconsolidated sands, SEG Annual Meeting, Expanded Technical Program Abstracts, 72, 1866-1869.

Zimmer, M., 2003, Controls on the Seismic Velocities of Unconsolidated Sands: Measurements of Pressure, Porosity and Compaction Effects, Ph. D. dissertation, Stanford University.

ABREVIATIONS AND ACRONYMS

Vp	Seismic P-wave velocity
Vs	Seismic S-wave velocity
Vclay	volume fracture of clay
ϕ	porosity
Nphi	neutron porosity
Q	sand point on plots
C	clay point on plots

DOE F 4600.6 (10-94) *Replaces EIA-459F* All Other Editions Are Obsolete	**U.S. DEPARTMENT OF ENERGY** **FEDERAL ASSISTANCE PROGRAM/PROJECT STATUS REPORT**	OMB Control No. 1910-0400

OMB Burden Disclosure Statement

Public reporting burden for this collection of information is estimated to average 47.5 hours per response, including the time for reviewing instructions, searching existing data sources, gathering and maintaining the data needed, and completing and reviewing the collection of information. Send comments regarding this burden estimate or any other aspect of this collection of information, including suggestions for reducing this burden, to Office of Information Resources Management Policy, Plans, and Oversight, Records Management Division, HR-422 - GTN, Paperwork Reduction Project (1910-0400), U.S. Department of Energy, 1000 Independence Avenue, S.W., Washington, DC 20585; and to the Office of Management and Budget (OMB), Paperwork Reduction Project (1910-0400), Washington, DC 20503.

1. Program/Project Identification No. **DE-FC26-04NT15506**	2. Program/Project Title **Imaging Reservoir Quality : Seismic Signatures of Geologic Processes**	3. Reporting Period **01/01/06** through **12/31/06**
4. Name and Address **Professor Gary Mavko (Research)** **Geophysics Department,** **Stanford University, 397 Panama Mall, Stanford, CA 94305-2215**		5. Program/Project Start Date **01/01/05** 6. Completion Date **12/31/08**
7. Approach Changes ☒ None		
8. Performance Variances, Accomplishments, or Problems ☒ None		

9. Open Items ☒ None	
10. Status Assessment and Forecast ☒ No Deviation from Plan is Expected	
11. Description of Attachments ☒ None	
12. Signature of Recipient and Date	13. Signature of U.S. Department of Energy (DOE) Reviewing Representative and Date

DOE F 4600.3A **OMB Control No.**

(09-92) **1910-0400**

U.S. Department of Energy
Milestone Log

OMB Burden Disclosure Statement

Public reporting burden for this collection of information is estimated to average 10 minutes per response, including the time for reviewing instructions, searching existing data sources, gathering and maintaining the data needed, and completing and reviewing the collection of information. Send comments regarding this burden estimate or any other aspect of this collection of information, including suggestions for reducing this burden, to Office of Information Resources Management, AD-241.2 - GTN, Paperwork Reduction Project (1910-0400), U.S. Department of Energy, 1000 Independence Avenue, S.W., Washington, DC 20585; and to the Office of Management and Budget (OMB), Paperwork Reduction Project (1910-0400), Washington, DC 20503.

Imaging Reservoir Quality: Seismic Signatures of Geologic Processes

Program/Project Title

Identification Number	Description	Planned Completion Date	Actual Completion Date	Comments
1	GEOLOGIC CONTROLS ON	12/31/06	12/31/06	Complete
2	QUANTIFY ELASTIC	12/31/06		ONGOING
3	SITE/DATA SELECTION	12/31/06	9/1/06	BEGINS YEAR 2
4	VALIDATION	04/30/08		BEGINS YEAR 3

ATTACHMENT A

Reservoir Quality Prediction by Integrating Sequence Stratigraphy and Rock Physics

(Presented at: Society of Exploration Geophysicists Annual Meeting, 2006 and Stanford Rock Physics Industrial Consortium Meeting, 2006)

SUMMARY

We present a methodology to improve the prediction of reservoir quality by combining principles of sequence stratigraphy and rock physics. The purpose of this study is to demonstrate how we can obtain critical sedimentological parameters and relative trends of their spatial variation from sequence stratigraphic interpretation. In turn, these sedimentological parameters can serve as constraints in rock physics modeling thereby reducing uncertainty in predicting reservoir properties from seismic amplitude.

INTRODUCTION

Sequence stratigraphy is the correct geologic interpretation of process/response events (Mulholland, 1998). This can predict the likely occurrence of reservoir facies, source rocks and seals. Traditional stratigraphic interpretation from post-stack seismic data has been predominantly qualitative based on visual inspection of geometric patterns in the seismic reflections. However, quantitative interpretation of seismic amplitude is possible if we can extract information about compositional maturity (mineralogy, clay content) and textural maturity (sorting, grain angularity, sphericity and roundedness) using principles of sedimentology.

Quantitative seismic interpretation (Avseth et al., 2005) uses rock physics to link seismic amplitude with reservoir properties, like, porosity, clay-content, sorting, diagenetic cements etc. However, one of the major sources of uncertainty in rock physics modeling arises due to our lack of knowledge about input parameters. This uncertainty can be reduced by constraining input parameters (for example, compositional maturity and textural maturity) as guided by sequence stratigraphic framework. Future developments of reservoir property prediction from seismic amplitude should benefit from close coupling between sequence stratigraphy and rock physics.

DEVELOPMENT OF CONCEPT AND METHODOLOGY

How can we obtain critical sediment parameters (and their spatial variation) from sequence stratigraphic interpretation and link them to seismic signatures? In the following section we outline the three main steps in our conceptual methodology. The next section applied these steps to a dataset from the Campos Basin. A workflow with the key steps is shown in Figure A-1.

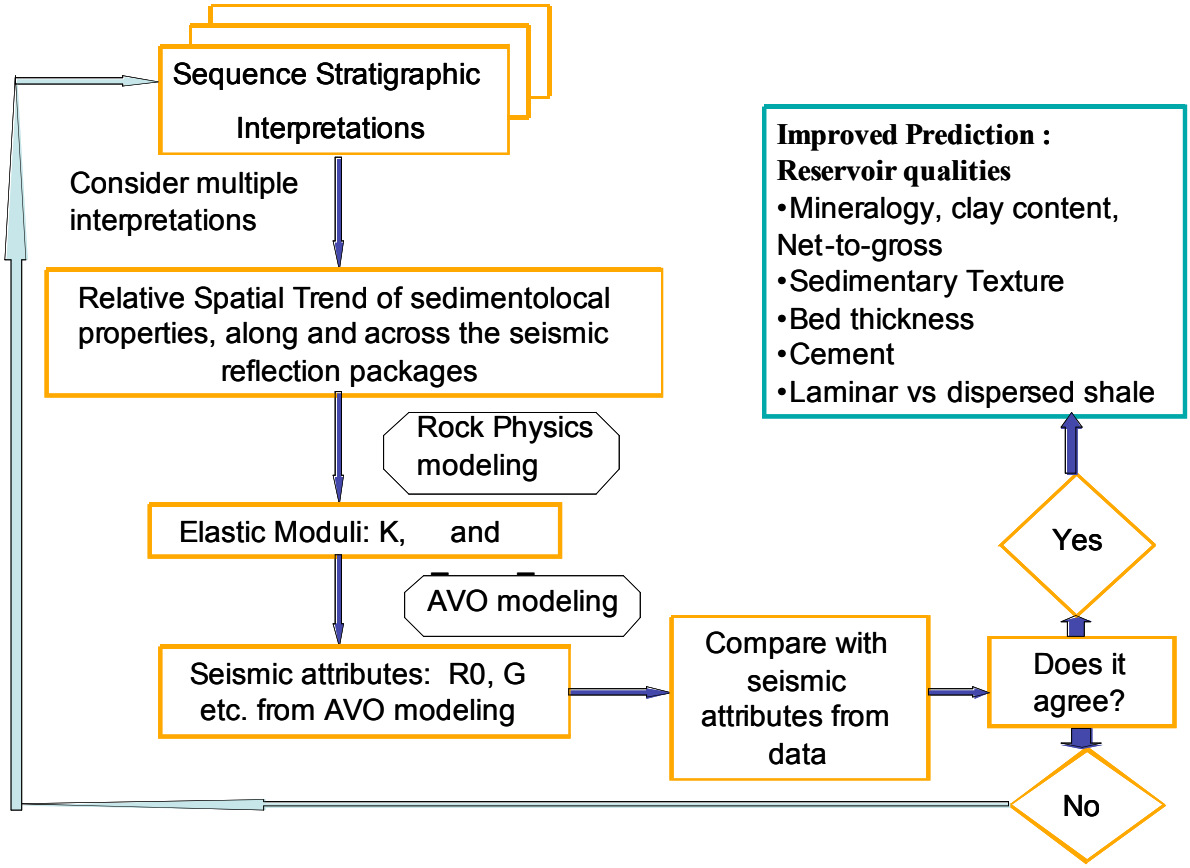

Figure A-1. Workflow for integrating sequence stratigraphy and seismic, using rock physics models.

Step-1A: Understanding the systematic change of sedimentological properties with depositional cycles in a predictable fashion

Wagoner et al. (1990) showed that the following sedimentological properties change predictably during transgression and regression:

- Sand-shale ratio
- Bed Thickness
- Grain-size
- Sorting
- Bio-turbation

Interestingly the changes in these sediment properties have opposite trends for transgression (shore line is approaching towards land) vs. regression (shore line is retreating towards basin). However there is uncertainty in these trends. During regression depositional energy tend to increase upward resulting in increase in bed-thickness, higher net-to-gross, better sorting and decrease in bio-turbation. On the other hand, marine transgression signifies decrease in depositional energy and exhibits an opposite trend of the above sediment parameters. These sediment parameters can be grouped as, compositional maturity and textural maturity parameters. They constitute important sediment properties that affect the elastic properties of the rocks and in turn affect seismic amplitudes.

Step-1B: Understanding spatial gradients of sedimentological properties

Gradients of sediment parameters are not same across the seismic reflector vs. along the reflector. Most seismic reflectors and their amplitudes correspond to chronostratigraphic surfaces with a few exceptions. Chronostratigraphic surfaces represent depositional hiatus. Changes in sedimentological properties are abrupt across the hiatus and gradual along the hiatus (Emery and Myers, 1996).

The spatial gradients can be calibrated from well data. Estimating the lateral trends requires multiple wells or horizontal wells. In the absence of such data one might assume that sediment parameters change linearly along the seismic reflector and in discrete steps across the reflector. Thus, using sequence stratigraphy, we obtain relative trends of variation in sediment properties within a depositional sequence. These trends then constrain the input parameters in rock physics modeling.

Step-2: Rock physics analysis

Rock physics establishes the relation between sedimentological properties and elastic moduli. After we determine the spatial trends of sediment parameters in a stratigraphic package, appropriate rock physics models are selected. The input parameters are guided by our results from step 1. The rock models are calibrated to well log data. As output we obtain effective bulk modulus, shear modulus and density, as well as Vp and Vs as a function of porosity.

Step-3: AVO modeling and interpreting seismic amplitude

AVO forward modeling (Shuey's approximation) is used to obtain intercept and gradient at key stratigraphic interfaces using effective moduli predicted from rock physics analysis in step 2. Trends in compositional and textural maturity are carried through from sequence stratigraphy, to the AVO plane, via rock physics. Finally, the modeling results can be used to interpret observed amplitudes in terms of sedimentological properties and reservoir quality.

EXAMPLE FROM CAMPOS BASIN, OFFSHORE BRAZIL

We have applied this concept in a deep-water turbidite system from Campos Basin, offshore Brazil. Sequence stratigraphic principles are less well-understood in deep water depositional system (Emery and Myers, 1996). Rock physics modeling can be useful tool to aid stratigraphic interpretations in deep-water systems. The facies package was deposited during low stand system tract (LST). Our interpretation was based on (a) basin history (Peres, 1990) (b) geometry and truncation patterns of reflectors (Figure A-2) and (c) stacking patterns of well logs (Figure A-3). The most likely depositional environment is submarine fan system.

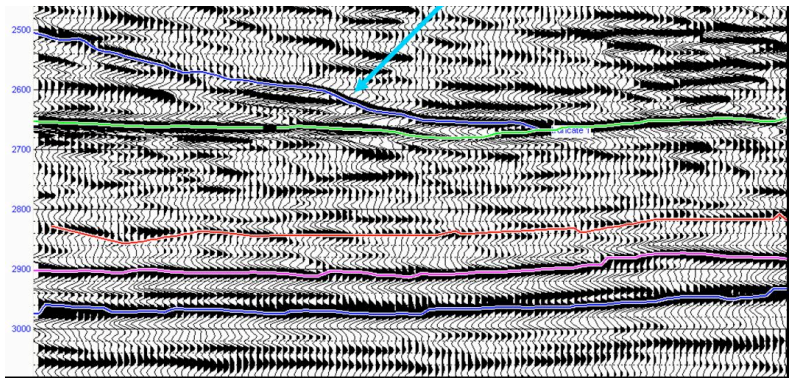

Figure A-2: The blue arrow indicates sub-marine fan system.

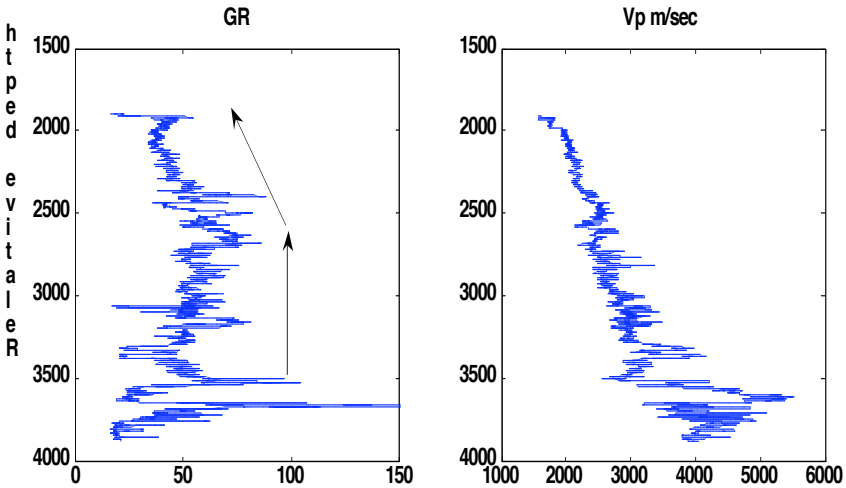

Figure A-3: In well log blocky motif corresponds to aggradational / channel deposits and coarsening-up motif corresponds to progradational depositional lobes.

We considered three para-sequences (PS) within the prograding depositional lobes (Figure A-4) and used sequence stratigraphic principles to obtain relative trend of sorting, an important parameter that controls porosity, elastic moduli, and hence seismic velocities. We create sorting trends as follows:

1. Sequence stratigraphic model from deep water prograding depositional lobes indicate that sorting increases vertically upward. Therefore we select lower PS to be poorly sorted, middle PS moderately sorted and the upper one is well sorted.

2. Laterally sorting improves linearly basin-ward within each para-sequence (Figure 4). Thin-section or core data available at any para-sequence could have verified or modified these sorting trends.

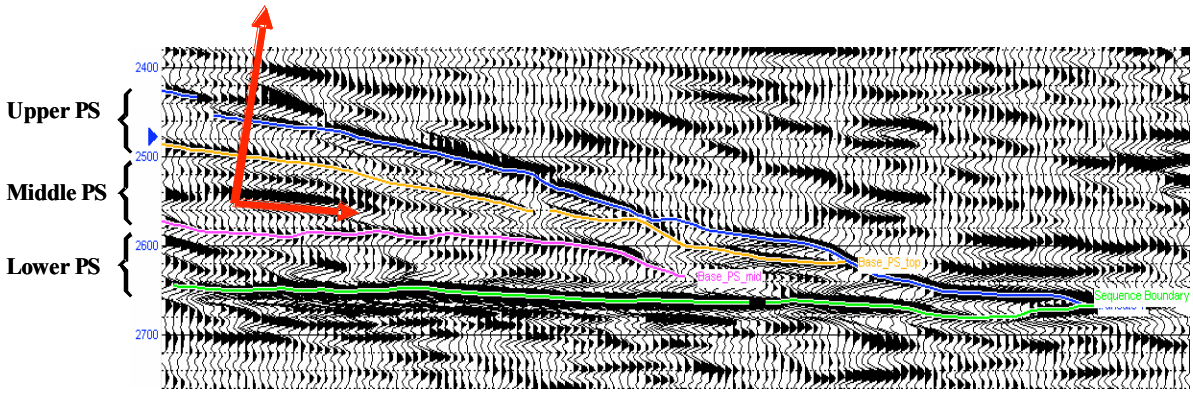

Figure A-4: Three parasequences (PS) interpreted within progradational depositional lobes. Changes in sorting is abrupt across the para-sequence boundaries and gradual along the boundaries.

We used experimental sorting-porosity relationship for artificially mixed sand (Beard and Weyl, 1973; Jorden and Campbell, 1984). Figure A-5 shows range of porosities for different sorting and various sandstone grain-sizes. Sorting is expressed in terms of the standard deviation of the distribution of the logarithm of the grain size. A plausible porosity section is shown in Figure A-6.

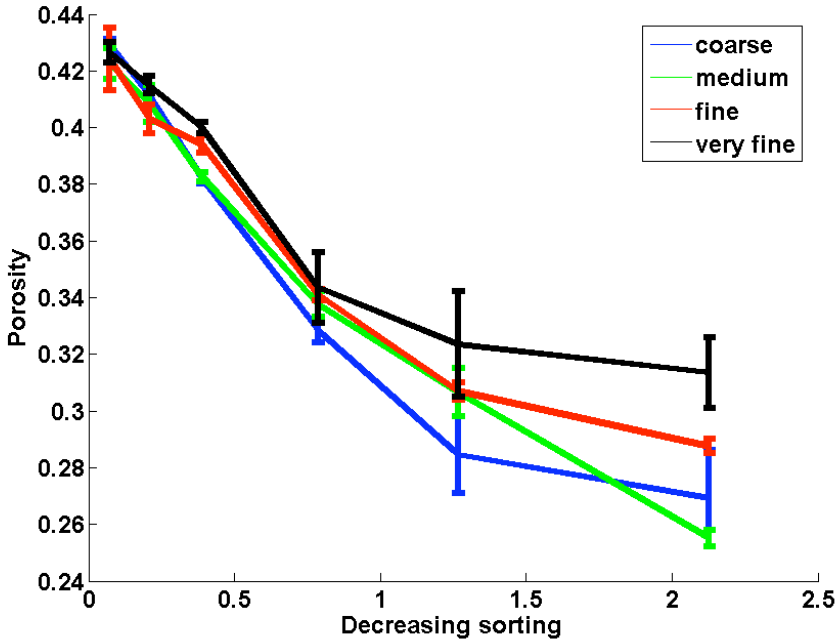

Figure A-5: Porosity decreases with detoriating sorting. Different curves represent different grain sizes in sandstone (Beard and Weyl, 1973; Jorden and Campbell, 1984).

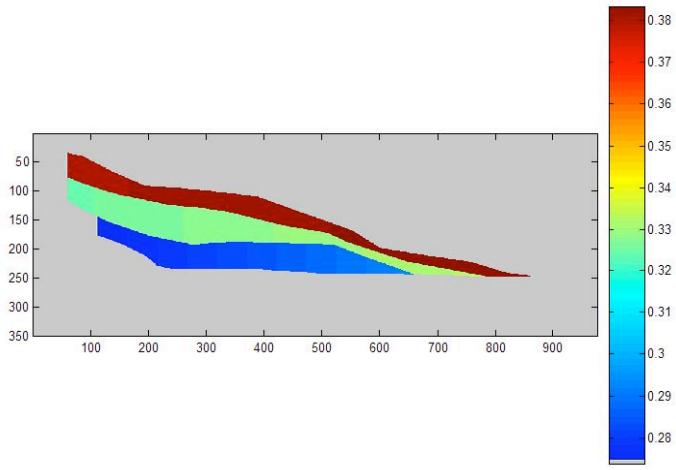

Figure A-6: Porosity section obtained using sorting-porosity relationship for artificially mixed sand.

The sandstones in submarine fans are compositionally immature. Therefore we used the unconsolidated sand model (Dvorkin and Nur, 1996; Mavko et al., 1998) with 80% quartz, 20 % feldspar and 10 % clay. A relatively lower quartz/ feldspar ratio indicates compositional immaturity. The unconsolidated sand model is used to compute elastic moduli of both well sorted and poorly sorted sands. Sorting detoriates from the well sorted end member as additional smaller grains fill the pore space. This increases the number of grain contacts and contact stiffness. The effective moduli at the well sorted, high porosity end member (~40%) are computed using Hertz-Mindlin (Mindlin, 1949) theory assuming coordination number (average number of grain contacts) of 6. Moduli of poorly sorted sand with porosities between 0 to critical porosity (~40%) are interpolated between mineral point and well-sorted end member using the lower Hashin-Shtrikman bound.

Figure A-7 shows porosities and velocities obtained from a neighboring well log and the predicted velocities using the unconsolidated sand model as described above. The Vp from well log is in good agreement with the model prediction. However the prediction for Vs is not good. To model spatial variation of effective moduli the porosity section from sequence stratigraphic interpretation is used as input to the calibrated rock model.

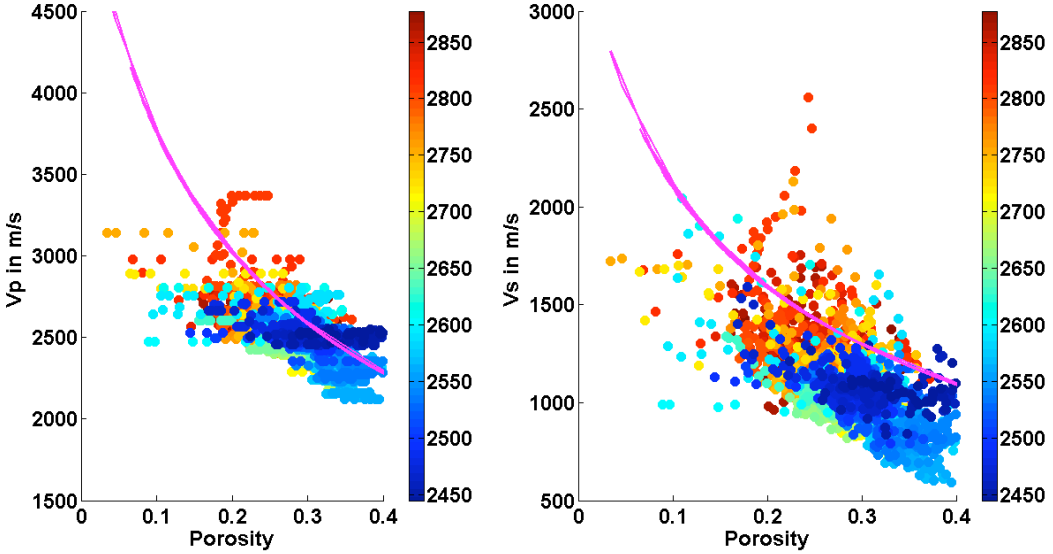

Figure A-7: The scatter points show measurements of porosities and velcities from well log in prograding lobes. The magenta line is obtained using rock physics modeling for unconsolidated sand.

The effective Vp, Vs, and density are used to compute intercept (R0) and gradient (G) at the interfaces of the three para-sequences. They indicate distinct trends in R0-G plane (Figure A-8). These trends can be used as a template to guide the interpretation of observed intercept and gradient from real seismic data. Since these trends incorporate the information from sequence stratigraphy, they can be used to predict the spatial variation in reservoir properties. But more than the qualitative trends, we can now make quantitative interpretations about porosity and sorting based on the calibrated rock model.

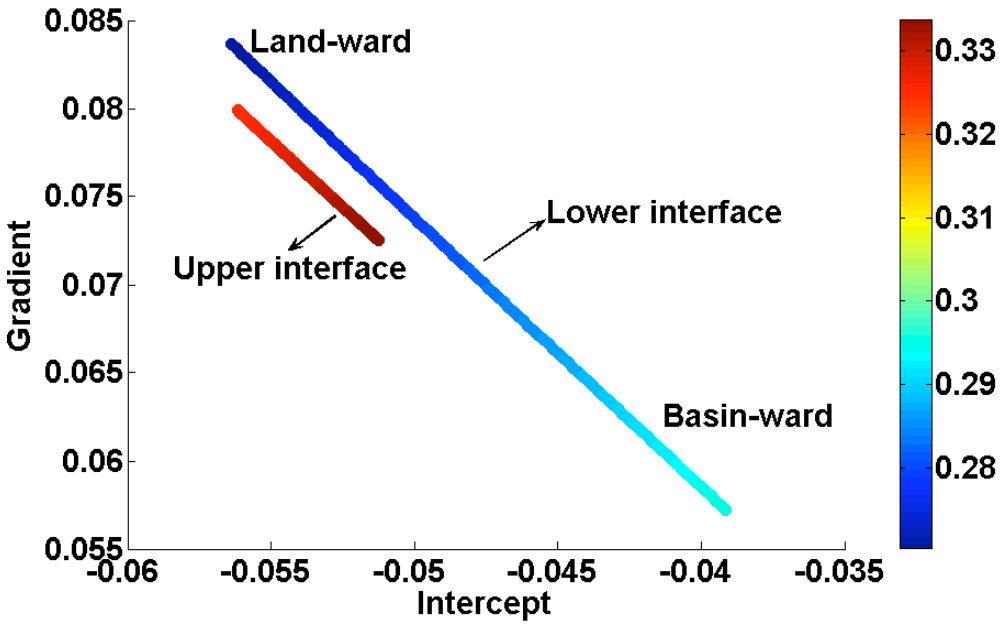

Figure A-8: AVO modeling results: Intercept and Gradient crossplot color-coded by porosity. They indicate distinct trend of variation in reservoir properties from landward to basin-ward.

In summary, we have developed a method to obtain spatial trends of sedimentological parameters from sequence stratigraphic interpretations. These trends are relative in a stratigraphic sequence. We have determined trends of grain-sorting in prograding lobes of submarine fan in Campos basin, Brazil using this method. However there is uncertainty in our interpretations since sequence stratigraphic principles are not very robust in deep water turbidite system. A further development to this workflow will be to consider multiple interpretations.

Rock physics modeling was constrained using trends of grain sorting as guided by sequence stratigraphic interpretations. In addition, the sands in submarine fan are compositionally less matured. Therefore the mineralogy was constrained by higher feldspar content.

The effective moduli computed from rock physics modeling were used to generate AVO attributes at two para-sequence boundaries. In R0-G plane we get linear trend of variation in sediment properties from landward to basin-ward. The trend indicates the mean of probability distribution of sedimentological properties and the variability will add scatter around this trend. Textural maturity progressively increases along this trend basin-ward. Furthermore since these trends are calibrated with the rock physics model it is possible to make quantitative interpretations about porosity and sorting. For example porosity progressively changes from ~31% to ~33% and ~27% to ~30% along upper and

lower interfaces respectively. The direct advantage of integrating sequence stratigraphy and rock physics is that seismic attributes (eg. intercept, gradient etc.) can be interpreted in terms of underlying sedimentological properties.

REFERENCES

Avseth, P., Mukerji, T., and Mavko, G., 2005, Quantitative Seismic Interpretation: Applying Rock Physics Tools to Reduce Interpretation Risk: Cambridge University Press.

Beard, D. C., and Weyl, P. K., 1973, Influence of texture on porosity and permeability of unconsolidated sand: American Association of Petroleum Geologists Bulletin, 57, 349-369.

Dvorkin, J., and Nur, A., 1996, Elasticity of high-porosity sandstones: Theory for two North Sea datasets: Geophysics, 61, 1363-1370.

Emery, D., and Myers, K., 1996, Sequence stratigraphy: Blackwell scientific publications, Inc.

Jorden, J. R., and Campbell, F. L., 1984, Well Logging I - rock properties, borehole environment, mud and temperature logging: Society of Petroleum Engineers (SPE) of American Institute of Mining, Metallurgical and Petroleum Engineers (AIME).

Marion, D., Nur, A., Yin, H., and Han, D., 1992, Compressional velocity and porosity in sand-clay mixtures, Geophysics, 57, 554-563.

Mavko, G., Mukerji, T., and Dvorkin, J., 1998, The Rock Physics Handbook, tools for seismic analysis in porous media: Cambridge University press.

Mindlin, RD, 1949, Compliance of elastic bodies in contact: ASME Journal of Applied Mechanics, 71, A-259 -268.

Mulholland, J.W., 1998, Sequence stratigraphy: basic elements, concepts and terminology: The Leading Edge, 17, 37-40.

Peres, W.E., 1990, Seismic-stratigraphic study of the Oligocene-Miocene shelf-fed turbidite systems of the
Campos Basin, Brazil: Ph.D. thesis, The University of Texas at Austin.

Stovas, A., Landrø, M., and Avseth, P., 2004, Estimation of net-to-gross and fluid saturation in a fine-layered sand-shale sequence – tested on offshore Brazil data: Society of Exploration Geophysicists International Exposition and 74th Annual Meeting, Expanded Abstracts, 228-231.

Wagoner, J.C.Van., Mitchum, R.M., Campion, K.M., and Rahmanian, V.D., 1990, Siliciclastic sequence stratigraphy in well logs, cores and outcrops: The American Association of Petroleum Geologists, Methods in Exploration Series, no. 7.

ATTACHMENT B

Sorting and Packing Effects on the Elastic Properties of Sands

Abstract

This section analyzes the effects of grain-size distribution (sorting) and packing on the porosity and elastic properties of granular materials, and how their effects differ. The effective medium contact theory for random packings of granular aggregates is used to approximate the effect of grain-size distributions. Based on that theory, an idealized model for tight (rhombohedric) packing of quinary mixtures is used to calculate the effective elastic properties of the aggregate, by performing stochastic simulations. The main source of uncertainty in these simulations comes from the coordination number. In spite of the approximations, the uncertainty in coordination number, and the limitations of using an idealized packing model, the results demonstrate that the sorting effect in the velocity-porosity plane follows a flatter trend than the modified Hashin-Shtrikman lower bound (MHSLB). In fact, the theoretical analysis demonstrates that the MHSLB should constitute an upper bound for the effect of sorting. On the contrary, the effect of packing can generate a trend with a steeper slope than the one predicted from the MHSLB. This steeper trend has been observed in laboratory studies and can be explained as the result of increasing grain-contact areas and incremental grain stabilization. Consequently, whereas the MHSLB is an approximate upper bound for the sorting effect, it should be considered a lower bound for the effect of packing. These conclusions are in agreement with results obtained from laboratory data in previous studies, and with subsurface core and well-log data.

The Rock-Physics Depositional Trend: Sorting or Packing?

Sandstones at similar depths or confining pressures present a relatively flat trend in the velocity-porosity plane (B-1). This flat trend results from significant changes in porosity associated with very small changes in elastic stiffness. The main porosity-reduction mechanisms related to this flat-trend are matrix (clay) content, sorting, and mechanical compaction, as shown by Marion *et al.* (1992), Avseth *et al.* (2000), Dvorkin

and Gutierrez (2001), Zimmer *et al.* (2002), and Zimmer (2003). For uncemented sandstones at the same pressure conditions, sorting and clay are considered to be the dominant mechanisms affecting this velocity-porosity trend. The trend can be reproduced using the modified Hashin-Strickman lower mound (MHSLB), and has been called the uncemented sandstone model (Mavko *et al.*, 1998), or the rock physics depositional trend (Avseth, 2000).

Grain-size distribution, or sorting, significantly affects not only the porosity (e.g. Beard and Weyl, 1973) but also the elastic properties of granular materials, as demonstrated by Estes *et al.* (1994), Avseth *et al.* (2000), Gutierrez and Dvorkin (2001), Gutierrez (2001), and Zimmer (2003). In spite of this importance, there are few experimental and theoretical studies about the effect of sorting. Dvorkin and Gutierrez (2001) present a model for binary mixtures that combines Hertz-Mindlin theory with modified Hashin-Shtrikman lower bounds to predict the elastic properties of the mixture. According to these authors, the sorting effect can be approximated using the MHSLB.

In the case of clean sand aggregates at similar pressure conditions, the uncemented trend is considered to be solely the effect of sorting (Avseth, 2000; Gutierrez, 2001). However, mathematical models of identical spheres demonstrate that a similar effect can be obtained by changing the packing of the aggregate, without increasing the confining pressure. Therefore, packing and sorting seem to have a similar effect on the velocity-porosity trend. The assumption that the uncemented trend is controlled by depositional factors (Avseth, 2000) disregards the effect of packing, which is often post-depositional. So far, there is not a physical explanation for the use of the MHSLB to model the effect of sorting. In addition to this, current rock physics models do not explain how we can distinguish between the sorting and packing effects on porosity and the elastic properties of granular aggregates.

Characterizing the effect of sorting on the elastic properties of granular materials can improve the methods to estimate and determine lithofacies and reservoir quality using sonic logs. The sorting effect can also be used to predict the variation in seismic response away from well control. Therefore, understanding the effect of sorting on the elastic properties of sands can help to assess the uncertainties associated with these predictions.

This section presents an analysis of the effects of grain-size distribution and packing on the elastic properties of granular materials, based on effective medium models. The next section discusses the measures of sorting or grain-size distribution, explains the relationships between porosity, sorting and packing, and their link to the depositional environments. After that, the following section reviews the aspects of the effective medium theories that are relevant to sorting and packing effects, and postulates some

approximations to account for the presence of different grain sizes in the contact models. The succeeding section introduces an old, idealized model for quinary mixtures. This model is used in the stochastic simulation of the effect of sorting on the elastic properties, explained in the section afterwards. The final sections show the comparison to real data, discuss the results and present the conclusions.

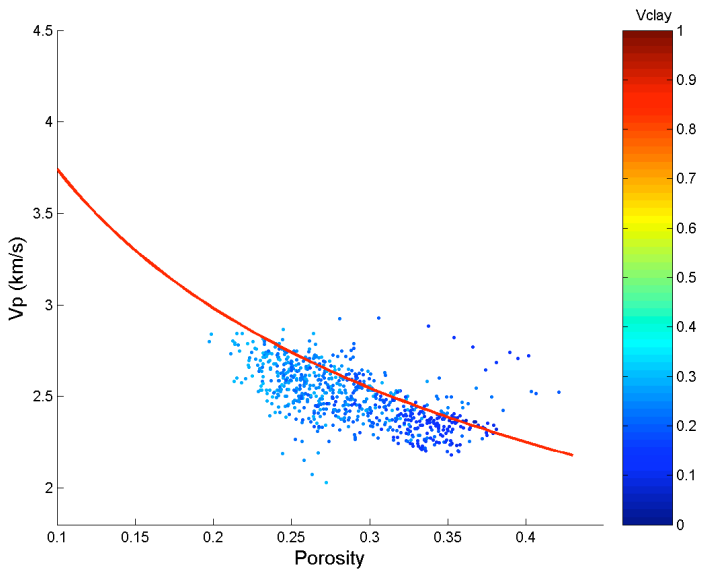

Figure B-1: The depositional trend of sands in the velocity-porosity plane. The data corresponds to uncemented sands from fluvial deposits (well Apiay-1). Data color-coded by clay fractio (Vclay).

Sorting, Packing, Porosity and Depositional Lithofacies

Sorting and packing are textural properties of the sediment, initially associated with the depositional processes. Sorting, or grain-size distribution, refers to the spread of the grain-size population. The grain size by itself is a measure of the center of that population. Packing refers to the grain concentration and is closely linked to porosity. Indeed, sorting, packing and porosity are closely related. The main textural components of sandstones are: grains, pores, matrix (clay), and cement (e.g. Selley, 1988). If we incorporate the matrix within the grain-size population, sorting and packing become the two dominant factors controlling porosity, and to some extent permeability, in uncemented sands. Permeability is linked to sorting and packing because of the effect of porosity, however permeability also depends on grain size and clay content.

Measures of Grain Size and Sorting

Grain size and sorting describe, respectively, the measures of the center and the spread of a grain population. In general, the grain size can be any measure of the population's center, either the mean, the median, or the mode, whereas sorting should be the respective measure of the population's spread, such as the standard deviation, the interquantile range, or the maximum absolute deviation. Although the application of these definitions to unconsolidated sands should be straightforward, there is no general agreement on which statistical parameters are the most appropriate measures, as explained below.

The grain size depends on the choice of the measure of the center. The logarithmic PHI scale was proposed by Krumblein (1936), as the most convenient scale to perform statistical analysis of grain-size distributions in sediments. As shown in Equation B.1, PHI is the negative, base-2 logarithm of the grain size in millimeters *(D)*. The classes are defined according to Wentworth's arithmetic scale (Wentworth, 1922). This usage conforms to the fact that most of the natural grain-size populations follow a log-normal distribution function. This fact introduces the first problem regarding the actual measure of the grain size: what is the right measure of the center, the mean or the median? For example, Pettijohn (1975) pointed out that sedimentologists commonly use the mode as the measure of grain size. Given that many populations show a lognormal distribution function, the median is probably the best measure of the center.

$$PHI = -\log_2(D)\,. \tag{B.1}$$

There is no unified measure of the spread of the grain-size distribution. Inter-percentile ranges in the PHI scale have been proposed as the most rigorous measures of sorting (Krumbein, 1938; Inman, 1956). However, the coefficient of variation (Equation B.2) is also a consistent measure of sorting. Authors proposing inter-percentile ranges have differed in the bounding percentiles: Krumbein (1936; 1938) proposed the interquartile range, which is equivalent to the sorting coefficient defined by Trask (1932); while Inman (1956), and Otto (1939), proposed the difference between the P_{84} and P_{16} percentiles. Some authors have found it convenient to normalize the inter-percentile ranges by the median (i.e. Rogers and Head, 1961). Sohn and Moreland (1968) used the coefficient of variation, defined as the standard deviation (σ) normalized by the mean (μ) of the grain-size distribution. Both methods of normalization provide consistent measures of sorting and are approximately equivalent. However, the coefficient of variation is preferable, since the normalized inter-percentile range presents the inconvenience of a singularity around grain sizes of 1 mm. Throughout this section we use the coefficient of variation as the Sorting Index (SI):

$$SI = \frac{\sigma}{\mu}. \tag{B.2}$$

Grain-size Distribution, Porosity and Permeability

Given a similar stage of packing, porosity of granular materials decreases as the standard deviation of the grain-size distribution increases. In other words, porosity decreases as sorting deteriorates (Figure B-2). This relationship has been demonstrated by various authors (Walton and White, 1937; Sohn and Moreland, 1968; Beard and Weyl 1973; and Zimmer, 2003). Other authors have observed a similar effect in binary mixtures (Fraser, 1935; Cumberland and Crawford, 1987), though they could not identify similar trends in multi-component mixtures. A linear trend between porosity and the sorting index can be derived from the published data (Figure B-3), which in general can be expressed as follows:

$$\phi = \phi_0 - \beta \frac{\sigma}{\mu}, \tag{B.3}$$

where ϕ_0 is the critical porosity of the aggregate, and the slope (β) has been found to vary between 0.11 and 0.19. The critical porosity, as defined by Nur *et al.* (1995), can be considered the well-sorted end member. Since porosity determines both the reservoir's final storage capacity and its permeability, grain-size distribution is therefore affecting both reservoir volumes and fluid flow in uncemented sand reservoirs. As can be observed in Figure B-4, the other property controlling permeability is the dominant grain size.

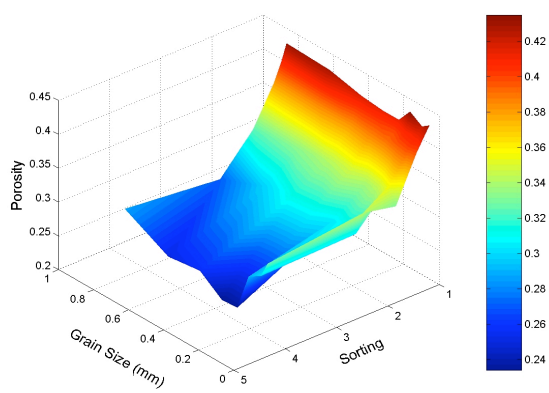

Figure B-2: Porosity of artificial sand mixtures as a function of grain size and sorting. Sorting is expressed as standard deviation. Based on data by Beard and Weyl (1973).

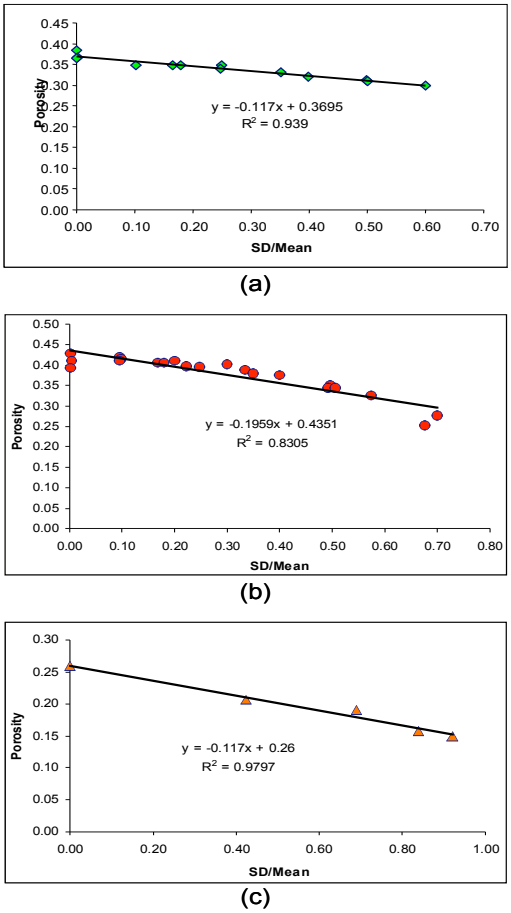

Figure B-3: Linear relationship between porosity and the sorting index σ/μ; (a) and (b) correspond to laboratory results published by Sohn and Moreland (1968); (c) corresponds to an idealized quinary mixture modeled by White and Walton (1937).

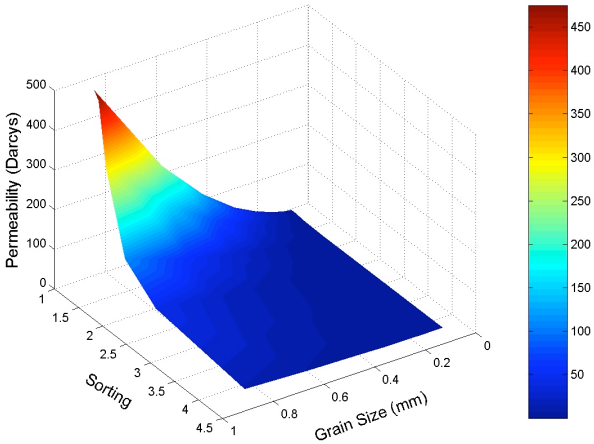

Figure B-4: Permeability of artificial sand mixtures as a function of grain size and sorting. Sorting is expressed as standard deviation. Based on data by Beard and Weyl (1973).

Sorting and Depositional Environments

Grain-size distributions reflect provenance, sediment-transport conditions, and the depositional process (Visher, 1999). According to Visher (1969), a grain-size distribution is composed of multiple log-normal populations. These populations are combined by multiple processes of sediment transport associated with traction, saltation and suspension, the three mechanisms of sediment transport in fluidized flows (e.g. Selley, 1988).

Visher (1969) divided the cumulative distribution function (CDF) of grain size, in the PHI scale, into three main components, each one corresponding to the main transporting mechanisms: traction, saltation and suspension (Figure B-5). The major truncation points occur about the transitional grain size values, which are those affected by two transporting mechanisms. These truncation points are defined as the 2-phi and the 3-phi break points. The former marks the transition between traction and saltation, and decreases in response to decreasing shear stress. The latter indicates the transition from saltation to suspension and decreases according to decreasing turbulence (Visher, 1999).

Although the relationship between sorting and depositional environments is not unique, grain-size distributions are always linked to the physics of the sedimentary processes. The non-uniqueness of sorting as an indicator of specific depositional settings derives from the fact that there are other variables involved, like provenance and sediment transport. Grain-size distribution depends not only on the specificities of the depositional setting, but also on the ability of the transporting current to separate different grain-size populations. Beach sediments, for example, are constantly reworked and sorted, therefore beach deposits tend to be well to very well sorted. However, if non-sorted sediments, like debris flows, are constantly discharged to the beach, then the most likely final result will be poorly to moderately sorted sediments. In spite of this non-uniqueness, the variations of sorting within a specific stratigraphic unit are always governed by the mechanics of sedimentation, as demonstrated by Inman (1949) and Visher (1969).

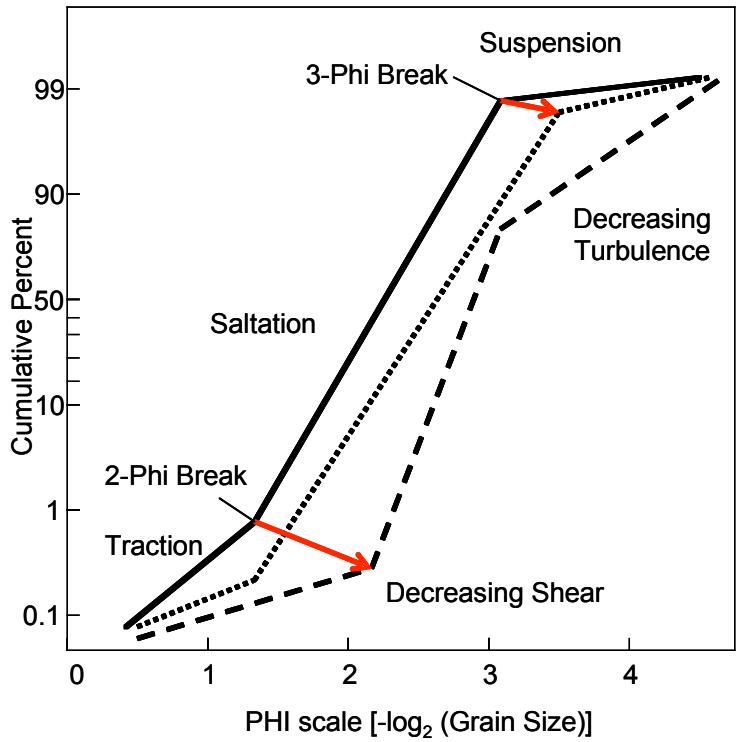

Figure B-5: Schematic cumulative frequency plots of grain-size distribution, illustrating the concept of the 2-phi and 3-phi breaks, and their general relationship with the mechanics of sedimentation according to Visher (1999).

Measures of Packing

Among several measures of packing the most common are the grain concentration, the coordination number (Allen, 2001), and the intergranular contact (Fuchtbauer, 1974). The grain concentration, or fractional volume concentration of particles (X), is directly related to porosity (ϕ):

$$\phi = 1 - X \qquad \text{(B.4).}$$

The coordination number (C), the average number of grains in contact with each individual grain, affects the stiffness of the aggregate. The intergranular contact describes the type of grain contact –punctual, tangential, concave-convex, or sutured–, and is usually a measure of the degree of mechanical compaction and pressure-solution, two processes related to diagenesis rather than to the depositional environment. According to Murphy (1982), and Zimmer (2003), porosity and coordination number can be related by the following expression:

$$C = 24e^{-2.547\phi} - 0.3731 \qquad \text{(B.5).}$$

However, there are other factors affecting porosity, like sorting (Beard and Weyl, 1973; Allen, 2001), grain shape (Allen, 2001), and grain angularity. Therefore the relationship between coordination number and porosity is not unique (Allen, 2001).

Table B.1: Main packing types for identical sphere packs (after Mavko *et al.*, 1998; Bourbie, 1987).

Packing Type	Porosity	Coordination Number	Comments
Cubic	0.476	6	Unlikely
Hexagonal	0.395	8	Lose
Rhombohedric	0.259	12	Tight
Random	~0.36	~9	Most Likely

Like sorting, packing has a strong effect on porosity and therefore on permeability. The relationship between packing, coordination number and porosity has been analyzed by several authors (Graton and Fraser, 1935; Bourbie *et al*., 1987; Murphy, 1982; Cumberland and Crawford, 1987). The effect of packing on both porosity and permeability was extensively analyzed by Graton and Fraser (1935). Murphy (1982) and Cumberland and Crawford (1987), identified the concomitant variation in both porosity and coordination number associated with changes in packing. For idealized packs of identical spheres these relationships are shown in Table B.1.

Packing and Depositional Environments

According to Allen (2001), laboratory experiments demonstrate that the conditions of deposition have a strong effect on the concentration of natural sediments. The results from different studies (Steinour, 1944; Kolbuszewski, 1948; Walker and Whitaker, 1967; and Macrae and Gray, 1961) indicate that the grain concentration varies from a constant value of about 0.65, comparable with that of dense haphazard packing, at small rate of deposition, to a lower constant value of about 0.55, comparable with that of loose haphazard packing, at higher rate of deposition.

A systematic relationship between depositional environments and packing has not been established. There are some general observations: e.g. clean turbiditic sands tend to preserve high porosities at significant burial depths in spite of having moderate sorting; beach deposits tend to have a tighter packing than fluvial point bars and therefore similar initial porosities, in spite of their better sorting. However, a systematic analysis does not exist. One reason might be that porosity variations associated with differences in packing

linked to the depositional environment are, in many cases, overprinted by mechanical compaction during the early stages of burial.

Incorporating Sorting into Effective-Medium Models

In order to take into account the effect of grain-size distributions on the effective elastic properties of granular material, our approach is to take the existing effective-medium models for uniform sphere packs, and modify them to incorporate the appropriate grain-size average. In other words, by finding the relevant averages of the variables involved in the computation, we can find approximate solutions to the effective elastic modulus. The following paragraphs will demonstrate that the appropriate averaging method varies, depending on the assumptions made during the derivation of each particular expression. For example, the harmonic average is the exact solution for the radius of curvature at the grain contact, whereas the average surface area requires a different averaging expression.

2.4.1. Contact Models

The starting point of effective-medium models based on contact mechanics is the solution of the normal and shear stiffness for two grains in contact. The following paragraphs outline this solution and explain the average required in the case of grains with different grain radii.

2.4.1.1 Radius of Grain-Contact Area

Timoshenko and Goodier (1956, p. 412) present the general solution for the pressure distribution within the contact area of two grains with identical elastic properties but different grain radii (R_1 and R_2). The radius of the surface of contact (a) is given by

$$a = \left(\frac{3}{4} \frac{F(1-\nu)}{G} \frac{R_1 R_2}{(R_1 + R_2)} \right)^{1/3} , \qquad \text{(B.6)}$$

where F is the force applied at the grain contact, ν is the Poisson's ratio of the mineral, and G is the shear modulus. This expression is equivalent to the following equation

$$a = \left(\frac{3}{8} \frac{F(1-\nu)}{G} R_c \right)^{1/3} , \qquad \text{(B.7)}$$

where

$$R_c = 2\left(\frac{R_1 + R_2}{R_1 R_2}\right)^{-1}. \tag{B.8}$$

Equation B.7 is general for isotropic, linear elastic grains and can be extended to the case of a small sphere in contact with a hypothetical sphere with infinite radius.

2.4.1.2 Normal and Shear Stiffness at the Grain Contact

Solutions for the normal stiffness of two grains in contact are presented by Mindlin (1949), Digby (1981), Walton (1987), and Johnson (1992), among others. Both normal and shear stiffness depend on the radius of the area of grain contact. The magnitude of this dependence varies with the loading sequence or the friction coefficient assigned to the grain surfaces. In general the normal stiffness is given by (Mindlin, 1949):

$$Sn = \frac{4aG}{1-\nu}. \tag{B.9}$$

The variation of the shear stiffness is more sensitive to the sequence of loading, the area of contact, and the friction coefficient. Different solutions to the shear stiffness have been given; in general they agree in proposing that the shear stiffness at the grain contact may vary from 0 to a maximum value given by

$$St = \frac{8aG}{2-\nu}. \tag{B.10}$$

Different mechanisms have been proposed to explain the variations in the shear stiffness at the grain contact. For example, Mindlin (1949) proposed that the controlling factor is the coefficient of friction, according to the expression:

$$St = \frac{8aG}{2-\nu}\left(1 - \frac{F_x}{\xi F_z}\right)^{1/3}, \tag{B.11}$$

where F_x and F_z stand for the shear and normal tractions at the grain contact, and γ is the coefficient of friction. From this equation it follows that if F_x equals the product ξF_z, then the shear stiffness is null. A similar model was proposed by Walton (1987). Digby (1981) related the shear stiffness to the pre-existing radius of the area of grain contact *(b)*, as follows:

$$St = \frac{8bG}{2-\nu}. \tag{B.12}$$

From this expression follows that if the pre-existing radius of the grain-contact area is close to zero, the initial shear stiffness is negligible. Null shear stiffness at the grain

contacts does not necessarily imply lack of rigidity of the aggregate. Bachrach (1998) associated variations in the rigidity of shallow unconsolidated sands with the proportion of null-shear-stiffness contacts.

2.4.1.3 Normal Force at the Grain Contact

Approximate solutions for the normal force at the grain contact are presented by Digby (1981) and Walton (1987). Digby (1981) demonstrates that the normal force is given by

$$F = \frac{4\pi R^2 P}{(1-\phi)C}, \tag{B.13}$$

where P is the applied hydrostatic pressure and ϕ is porosity. R and C stand for the sphere radius and the coordination number, respectively. According to Digby (1981), this result agrees exactly with the solution for different grain sizes obtained by Brandt (1955). This expression is also equivalent to the equations presented by Walton (1987). The expression $4\pi R^2$ represents the surface area of each identical sphere. For varying grain sizes, the normal force at the grain contact becomes a function of the average grain surface area (S_{avg}) and the grain coordination number (C_g).

2.4.1.4 The Coordination Number of a Binary Mixture

The average coordination number of a mixture (C_{avg}) increases as sorting deteriorates; however the variation of C_{avg} in binary mixtures is not linear and reach an upper limit as the number of small spheres, with low coordination number, increases. This is because the average coordination number depends not only on the number of grains per volume, but also on the volumetric average of grain sizes. The maximum number of small spheres (C_{big}), of radius R_{small}, surrounding a bigger sphere, of radius R_{big}, depends on the ratio between the total surface area around the big sphere, and the area of a circle of radius R_{small}. This maximum coordination number can be approximated by the following expression:

$$C_{big} \approx \frac{3}{4}\left[4\left(\frac{R_{big}^2}{R_{small}^2} + 2\frac{R_{big}}{R_{small}} + 1\right)\right]. \tag{B.14}$$

The fraction (3/4) has been introduced to fit the maximum coordination number of identical spheres to 12, instead of 16. Assuming C_{small} as the average coordination number for the small spheres, where $C_{small} \leq C_{big}$, the average coordination number of the whole aggregate is:

$$C_{avg} = \frac{\#Contacts}{\#Spheres} = \frac{AC_{big} + AC_{big}C_{small} + ABC_{big}C_{small}}{A + AC_{big} + ABC_{big}}, \tag{B.15}$$

where A is the total number of spheres, and B is the proportion of small spheres that are not in contact with the big spheres. Figure B-6 illustrates the results obtained from Equations B.14 and B.15, taking A = 8, and different values for C_{small} and B. It clearly shows that the ratio between C_{avg} and C_{big} rapidly decreases to almost zero, as the ratio of R_{big} to R_{small} increases. Meanwhile the ratio of C_{avg} to C_{small} increases and exponentially reaches an upper limit, where C_{avg} is slightly larger than C_{small}.

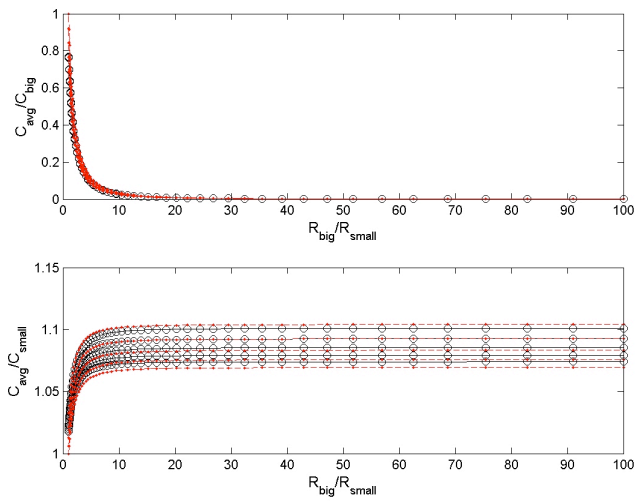

Figure B-6: Variation of C_{avg} as the ratio between R_{big} and R_{small} increases (sorting deteriorates). For large values of R_{big}/R_{small}, C_{big} is much larger than both C_{small} and C_{avg}. C_{avg} increases as sorting deteriorates; however it rapidly reaches an upper limit slightly larger than C_{small}.

2.4.1.5 The Softening Effect of Variable Grain Size

Putting small spheres in between larger spheres has a softening effect on the elastic modulus of sphere packs. This can be mathematically demonstrated throughout the analysis of uniaxial deformation of three grains in contact, based on the sketch shown in Figure B-7. The elastic modulus (M_1 and M_2) for the uniaxial deformation of the two configurations shown in Figure B-7 are given by

$$M_1 = \frac{\partial P}{\varepsilon_1} = \frac{L_1}{\partial\delta_0 + \partial\delta_1}\partial P, \tag{B.16}$$

$$M_2 = \frac{\partial P}{\varepsilon_2} = \frac{L_2}{\partial\delta_0 + \partial\delta_2}\partial P. \tag{B.17}$$

where ε_1 and ε_2 are the respective uniaxial strains. To demonstrate that M_1 is also larger than M_2 we need to prove that $\Delta\delta_1$ is smaller than $\Delta\delta_2$, since L_1 is larger than L_2. For any grain contact $\Delta\delta$ is given by (i.e. Mavko *et al.*, 1998)

$$\partial\delta = \frac{\partial F}{Sn}. \tag{B.18}$$

Considering that the force at the grain contacts is the same, and recalling equations B.6 and B.9, it follows that Sn_1 is larger than Sn_2 and consequently:

$$\partial\delta_1 = \frac{\partial F}{Sn_1} < \frac{\partial F}{Sn_2} = \partial\delta_2 . \tag{B.19}$$

Therefore M_1 is larger than M_2.

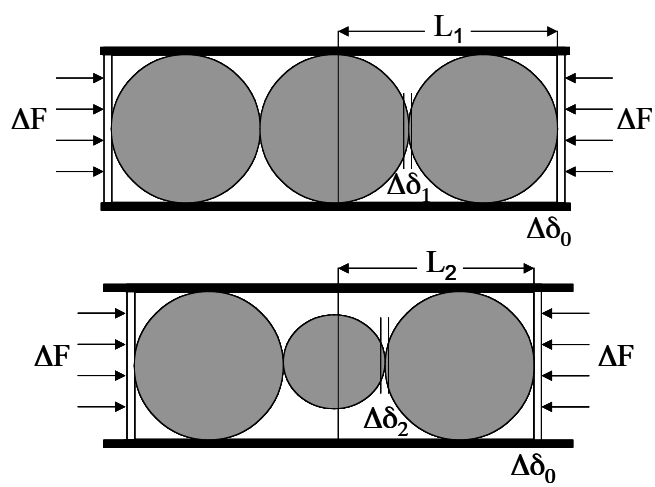

Figure B-7: Sketch for the analysis of uniaxial deformation of three grains in contact.

2.4.1.6 Effective Elastic Modulus of Sphere Packs with Variable Grain Size

Winkler (1983) demonstrated that the general solutions for the effective elastic properties of random packs of identical spheres, derived by Digby (1981), are not specific to Digby's model and can be generalized to different contact models. From Digby's derivation, the effective elastic properties of a random packing of spheres is given by (Winkler, 1983):

$$Keff \approx \frac{C(1-\phi)}{12\pi R} Sn , \tag{B.20}$$

$$Geff \approx \frac{C(1-\phi)}{20\pi R}\left(Sn + \frac{3}{2} St \right). \tag{B.21}$$

To incorporate the effect of grain-size distribution into these models, grain radius *(R)*, coordination number *(C)*, normal stiffness *(Sn)*, and shear stiffness *(St)* are replaced in the expressions above for their equivalent averages. Then we can rewrite the previous equations:

$$Keff_{sort} \approx \frac{C_{avg}(1-\phi)}{12\pi R_{avg}} Sn_{avg} \ , \tag{B.22}$$

$$Geff_{sort} \approx \frac{C_{avg}(1-\phi)}{20\pi R_{avg}} \left(Sn_{avg} + \frac{3}{2} St_{avg} \right). \tag{B.23}$$

These equations can be used as a first approximation to model the effect of sorting on the effective elastic properties. The question is then, which are the appropriate averages to use?

2.4.1.7 What are the Appropriate Averages?

The averages required refer to either the local average for two grains in contact, or the global average of the aggregate. Whereas the different averages for sphere radii have an exact solution, the averages for coordination number and the average ratio *a/R* are inferred. For example, the harmonic average for the radius of curvature for two grains in contact is exact (Timoshenko and Goodier, 1956). For a sphere configuration like that shown in Figure B-8, the different averages are indicated in Table B.2.

It becomes clear, by looking at Table b.2, that variable sphere sizes in contact require the evaluation of different average radii for each expression. The best example is the difference between the local average radius of curvature (*Rc*) and the average grain radius required for the average surface area (R_{avg}). The former requires the harmonic average of the sphere radii in contact, whereas the later average is given by the following expression:

$$R_{avg} = \left(\sum_k f_k R_k^2 \right)^{1/2} \tag{B.24}$$

These two are exact results. Another difference seems to exist between the local radius of curvature and the global average sphere radius (*Rg*). Either the arithmetic average or the geometric average is proposed for *Rg*. The arithmetic average provides the best results during stochastic simulation, since enhances the softening effect of variable grain sizes. However a rigorous justification of its use is lacking. It is important to point out that coordination numbers vary within a small range; therefore the different choices of

averages for local and global coordination numbers do not have a dominant effect in the final result. Notice also that all these expressions reduce to the Hertz-Mindlin model when we consider identical spheres. They will also reduce to Hertz-Mindlin expressions if we use the harmonic average for local radius of curvature, average sphere radius, and average surface area.

The expressions presented in Table B.2 imply that introducing small spheres between the contacts of larger spheres may actually decrease the aggregate stiffness. Although this effect might not be intuitively obvious, it agrees with the fact that the area of grain contact is controlled by the radius of the small sphere, whereas the average sphere radius is dominated by the large sphere. This softening effect of small spheres is comparable to the effect of grain angularity analyzed by Bachrach *et al.* (2000).

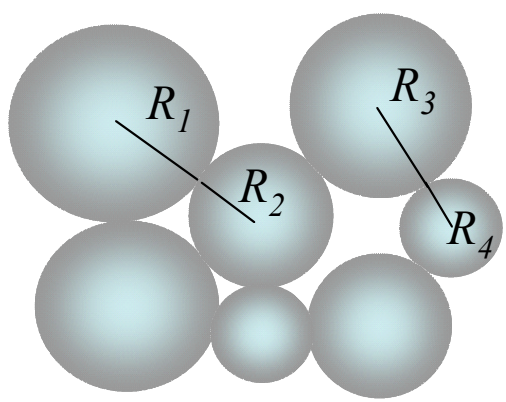

Figure B-8: An aggregate of spheres with variable radii.

Table B-2: Summary of equations and variables used to incorporate variable sphere radii into effective-medium contact models.

Variable	**Expression**	**Reference or Assumption**
Local grain-contact area between R_i and R_j	$a_{ij} = \left(\frac{3}{8} \frac{F_{ij}(1-\nu)}{G} Rc_{ij} \right)^{1/3}$	Timoshenko and Goodier (1956)
Local radius of curvature of R_i and R_j	$Rc_{ij} = 2\left(\frac{R_i + R_j}{R_i R_j} \right)^{-1}$	Timoshenko and Goodier (1956)
Local coordination number	$C_{ij} = 2\left(\frac{1}{C_i} + \frac{1}{C_j} \right)^{-1}$	*C* controlled by the weakest contact

Volumetric average radius	$R_e = \left(\sum_k f_k R_k^3 \right)^{1/3}$	Exact solution for the average volumetric radius.
Global average surface area	$S_{avg} = 4\pi \sum_k f_k R_k^2$	Exact solution for the average surface area.
Intergranular force between R_i and R_j	$F_{ij} = \frac{S_{avg} P}{C_{ij}(1-\phi)}$	Digby (1981)
Global average ratio $\alpha = \frac{a}{Rg}$	$\alpha_{avg} = \sum_k f_k \alpha_k$; where: $\alpha_k = \frac{a_{ij}}{Rg_{ij}}$	*Rg* differs from the radius of curvature and corresponds to the global volumetric average radius
Global average coordination number	$C_{avg} = \sum_k f_k C_k$	C_k varies between 6 and 12
Effective Bulk Modulus	$Keff_{sort} = \frac{C_{avg} G(1-\phi)}{3\pi(1-\nu)} \alpha_{avg}$	Generalized Hertz-Mindlin for average *C* and α

2.4.2. The Modified Hashin-Shtrikman Lower Bound (MHSLB) and Sorting

The MHSLB can be considered an upper bound for the sorting effect on the elastic properties of granular materials. Dvorkin and Gutierrez (2001) used the MHSLB to model the effect of sorting in unconsolidated sandstones, based on the theoretical analysis and experimental results for binary mixtures. Although a good approximation, the use of binary mixtures and the MHSLB to estimate the effect of variable grain size does not take into account the softening effect of introducing small spheres between large spheres. As a result of the variable grain size, the normal and shear stiffness at these contacts decrease, resulting in an effective elastic modulus lower than that predicted from the MHSLB. Recent laboratory studies by Zimmer (2003) show that the effect of sorting follows a flatter trend than the one predicted by the MHSLB (Figure B-9). Consequently, the MHSLB provides a stiffer estimate of the actual impact of varying grain size, and constitutes an empirical upper bound for the concomitant effect of sorting on the elastic properties and porosity of granular materials.

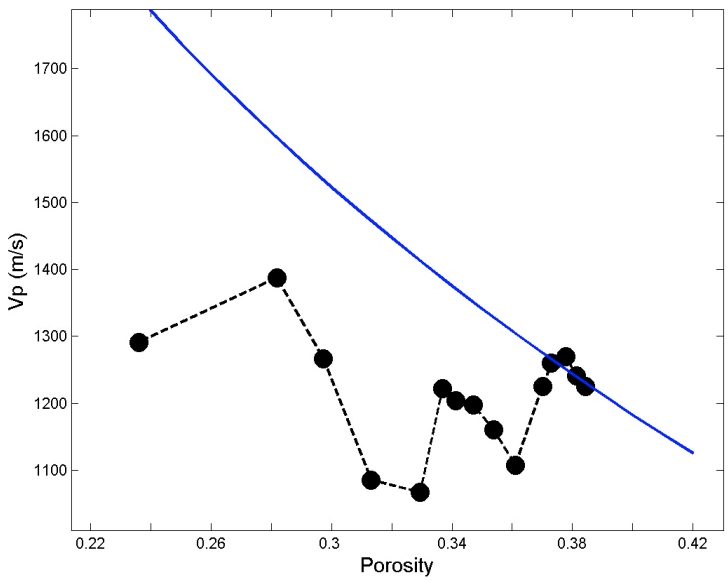

Figure B-9: Sorting trend for six different sand aggregates, with variable sorting, at 5 MPa confining pressure (after Zimmer, 2003). The large variations in porosity are related to the changes in sorting. The blue line corresponds to the Hashin-Strickman lower bound, after fitting the first data value. Notice the flat and irregular trend associated with the variations in sorting.

Modeling the Effect of Packing

In the case of idealized spheres, the main effects of grain rearrangement are reducing porosity and incrementing coordination number, as shown in Table B.1. Other possible additional effects involve grain stabilization and change in the grain-contact area. The packing effect can be modeled using either Hertz-Mindlin contact theory or the MHSLB. In both cases, the modeling results underestimate the increase in elastic stiffness associated with packing, as observed in laboratory analysis (Zimmer, 2003). Hertz-Mindlin and MHSLB models provide similar results, both neglecting the impact of grain stabilization and local increase in grain-contact area. From this analysis it follows that the MHSLB constitutes a lower bound for the packing trend in the velocity-porosity plane. Consequently, it also constitutes an empirical lower bound for the overall effect of mechanical compaction on the elastic properties of granular materials.

2.5.1. Modeling the Packing Effect with Hertz-Mindlin Theory

The pure packing effect obtained from the Hertz-Mindlin model underestimates the slope observed in laboratory data, as shown in Figure B-10. Hertz-Mindlin theory for the elastic properties of granular materials is summarized in Equations B.6 to B.13, and

Equations B.20 to B.21. As documented by Mavko et al. (1998), for identical spheres the model becomes independent of the sphere radius. Besides the elastic properties of the minerals (G and v) and the confining pressure (P), the dominant parameters become the grain-contact area (a), porosity (ϕ) and coordination number (C). For the case of ideal spheres, the change in grain-contact area is exclusively associated with confining pressure, because the grains do not have rectilinear faces. Therefore, the only variables controlling the change in elastic properties associated with grain accommodation are porosity and coordination number. To use Hertz-Mindlin theory to model the packing effect, the mutual change of porosity and coordination number can be estimated from Murphy's relationship (Equation B.5). Figure B-10 compares the trend obtained from Hertz-Mindlin model, with the trend observed from laboratory results (Zimmer, 2003). An assumption of no shear stiffness at the grain contacts was necessary to match the laboratory data. The slope of the data is slightly larger than the slope obtained from the Hertz-Mindlin model.

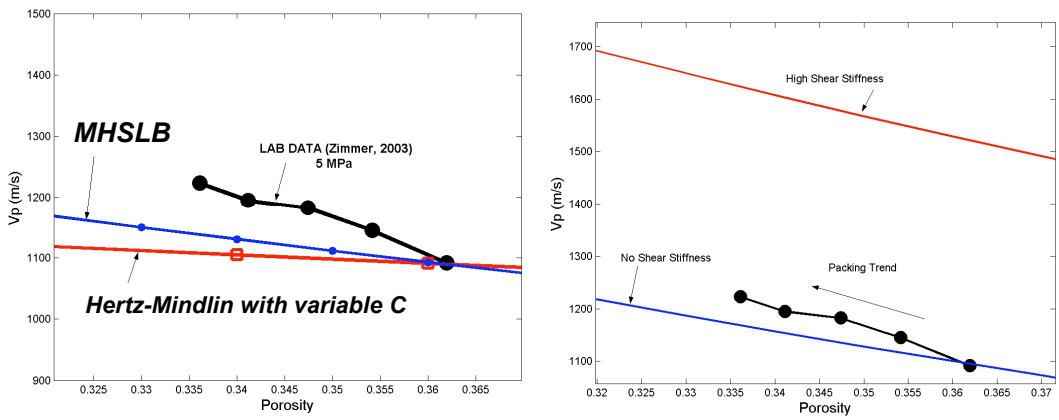

Figure B-10: Comparison between laboratory results showing the effect of packing (Zimmer, 2003), and the modeled effect of packing using the modified Hashin-Shtrikman lower bound (MHSLB), and Hertz-Mindlin (HM) theory combined with Murphy's relationship for *C* and ϕ (Eq. B.5). Figure on the left shows the results for the Unconsolidated Sandstone Model (Mavko, et al., 1998), which combines both the HM theory (for the anchor point) and the MHSLB. The red line shows that HM theory overestimates the velocity for unconsolidated sands. To fit the data, a correction factor for shear stiffness is necessary. The slope of the packing trend is slightly but systematically steeper than the MHSLB.

Another effect associated with mechanical compaction is grain stabilization (i.e. Zimmer, 2003). Laboratory and field studies of unconsolidated sandstones at low confining pressure demonstrate that to fit the data, low or no shear stiffness at the grain contacts has to be assumed (Bachrach, 1998; Zimmer, 2003). This discrepancy has been explained as the result of grain angularity (Bachrach, 1998) and grain sliding or rolling

(Zimmer, 2003). On the other hand, Avseth (2000) and Gutiérrez (2001) have successfully used Hertz-Mindlin to model velocities of friable (uncemented) sandstones at depth. This discrepancy suggests that there is a compaction stage at which grain sliding or rolling is no longer feasible because of tight packing, and therefore the assumptions of the Hertz-Mindlin theory become valid. Figure B-10 illustrates the difference between the assumptions of no shear stiffness and high shear stiffness at the grain contacts.

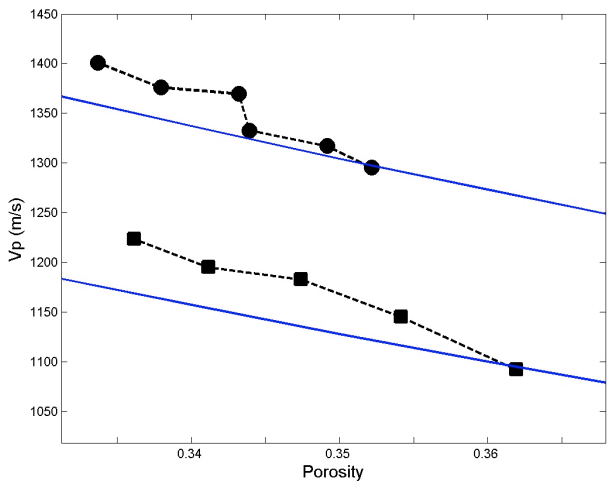

Figure B-11: Compaction trend for a sand aggregate at 5 and 10 MPa confining pressures, after different loading cycles (Zimmer, 2003). The blue curves are the Hashin-Strickman lower bounds, after fitting the first data point. Notice the steeper slope of the compaction trend.

2.5.2. The Modified Hashin-Shtrikman Lower Bound and Packing

The comparison of the packing trend obtained from the MHSLB and laboratory results (Figure B-11), shows that the MHSLB underestimates the effect of packing. The packing trend obtained from the MHSLB is about the same as that obtained from the Hertz-Mindlin model (Equations B.7, B.9, B.10, B.13, B.20, and B.21). The trends obtained from Hertz-Mindlin theory and MHSLB do not account for the effect of grain stabilization. In addition to this, the Hertz-Mindlin theory assumes idealized spheres that do not increase the grain-contact area after grain rearrangement These two factors will increase the aggregate's elastic modulus, as the steeper slope of the laboratory data indicates. Consequently, both the Hertz-Mindlin model and the MHSLB constitute lower bounds for the effect of grain accommodation on both porosity and the elastic properties of granular materials. In particular, the MHSLB can be considered a lower bound for the effect of mechanical compaction.

An Idealized Quinary Mixture

In order to mathematically evaluate the effect of sorting, we use a model for gradual infilling of a tight rhombohedric packing of spheres developed by White and Walton (1937). These authors calculated the size and the number of gradually smaller spheres required to fill the spaces between larger spheres. Starting from the tight packing of identical spheres, they made the analysis for five different sphere sizes forming a quinary mixture (Table B.3). They also calculated the porosity reduction and the increment in surface area, as the mixture changed to binary, ternary, quaternary and quinary. The sorting index for each mixture has been derived from their results. Table summarizes their results, and includes the sorting index of these mixtures. In spite of its idealized rhombohedric packing, White and Walton's study gives us the basic information to calculate the effect of sorting using the equations in Table .

Table B.3: Parameters for the groups of infilling spheres for a rhombohedric packing (after White and Walton, 1937). The first column corresponds to the rhombohedric packing of identical spheres. The following columns indicate the size and volumes of the infilling spheres, and the final volume, porosity, surface area and sorting index of the resulting mixture.

	1st	**2nd**	**3rd**	**4th**	**5th**	**Filler**
Radius	r	0.414r	0.225r	0.177r	0.116r	Very small
Relative # of spheres	1	1	2	8	8	
Volume	$4.189r^3$	$0.298r^3$	$0.0476r^3$	$0.0225r^3$	$0.0066r^3$	
Added volume	$4.189r^3$	$0.298r^3$	$0.0952r^3$	$0.180r^3$	$0.0526r^3$	$0.622r^3$
Total volume of spheres	$4.189r^3$	$4.487r^3$	$4.582r^3$	$4.762r^3$	$4.815r^3$	$5.437r^3$
Porosity	0.2595	0.207	.19	0.158	0.149	0.039
Surface area	$12.566r^2$	$14.732r^2$	$16.004r^2$	$19.080r^2$	$20.456r^2$	
Sorting Index (SD/mean)	0.0	0.42	0.69	0.84	0.92	

Stochastic Simulation of Effective Elastic Properties

In order to evaluate the effect of grain-size distribution we use the quinary-mixture model from White and Walton (1937), and perform stochastic simulations using the equations in Table B.2. The input parameters for this algorithm are the grain-size distributions, the porosity, the coordination numbers for each grain size, and the elastic properties of the solid. The grain-size distributions vary as we add smaller fractions to the aggregate, starting from identical spheres (1st column in Table B.3), and then adding

smaller spheres: 2nd column for a binary mixture, 3rd column for a ternary mixture, and so on. For each case we modeled a mixture with 2400 grains. The coordination numbers for the larger spheres increase as we add smaller spheres, reaching a top value of 19, under the assumption that all the added spheres are in contact with the largest spheres. However the coordination number of the added smaller spheres is always low (6-9). The harmonic average for the local C_{ij} was used in order to give more weight to the small sphere's C.

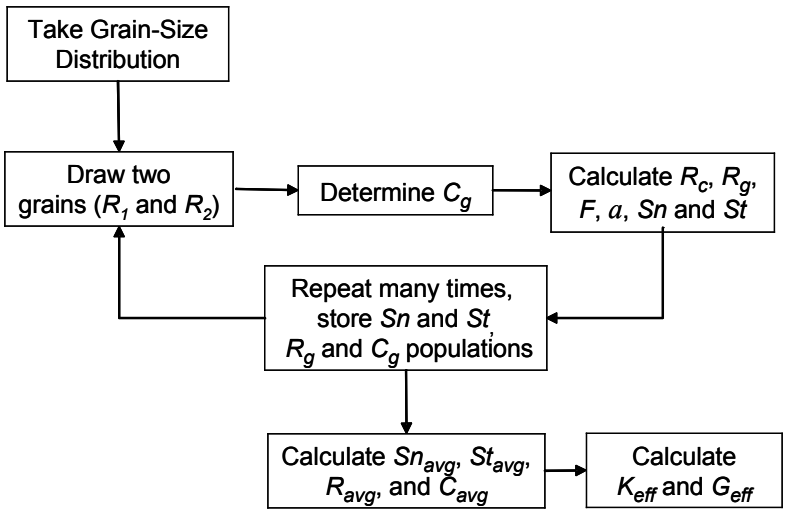

Figure B-12: Algorithm to evaluate the effect of grain-size distribution on elastic properties, using stochastic simulation. C_g, R_c, and R_g are the averages of coordination number, radius of curvature and grain radius at each grain contact; F, a, Sn and St are force, radius of grain contact area, normal and shear stiffness at each grain contact. Sn_{avg}, St_{avg}, R_{avg}, and C_{avg} are the global averages of normal and shear stiffness, grain radius, and coordination number.

The algorithm steps are schematically shown in Figure B-12, and the green lines in Figure B-13 outline the results obtained from this algorithm. For every grain-size distribution, each grain size has a specific coordination number; therefore the coordination number at each grain contact (C_{ij}) is determined from the drawn grain radii R_i and R_j. The global averages of grain radius and coordination number are calculated from the populations Rg_{ij} and C_{ij}. To evaluate the uncertainty associated with the which local and global coordination numbers are appropriate, additional simulations were performed using different options for the global (C_{avg}) and local (C_{ij}) coordination numbers. The results, also shown in Figure B-13, indicate a variation from 10% to 16% for a given grain-size distribution, specified by porosity and sorting. As expected, the assumption of constant C_{avg} and C_{ij} generates the lowest variability. Remarkably, the algorithm outlined in Figure B-12 produces an irregular trend similar to the one observed in the laboratory data.

The range of variability obtained from the stochastic models is small, and outlines a velocity-porosity trend flatter than the one predicted from the MHSLB. Fluid substitution puts the results within the framework of the well-established rock physics depositional and diagenetic trends. The final results are shown in Figure B-14. Within this framework, it is clear that the scatter introduced by the uncertainty of the coordination number is relatively small, and all the different results follow a relatively flat trend. Using the highest-porosity value as the anchor point, it is clear that the results from the stochastic simulations follow a flatter trend than the MHSLB.

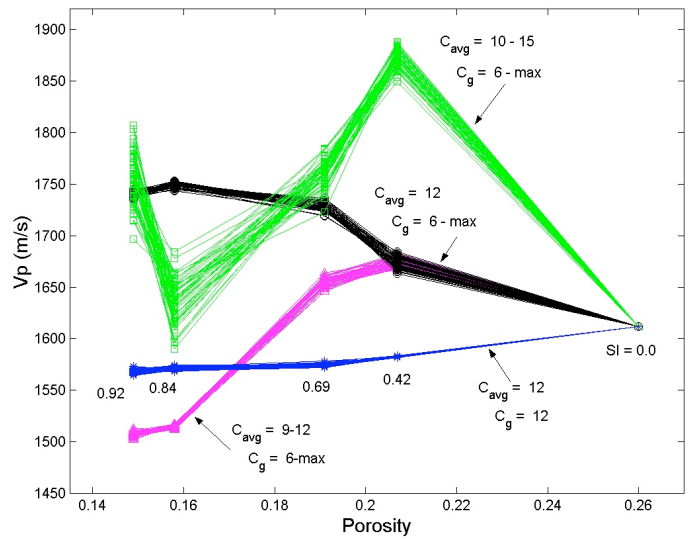

Figure B-13: Results from the stochastic simulation. The green line corresponds to the algorithm outlined in Figure B-16. SI corresponds to the sorting index for each grain-size distribution (Equation 2). The other lines show results from different simulations, assuming C_{avg} either is 12 or varies from 9 to 12, and C_g either is 12 or varies from 6 to the maximum possible for each mixture.

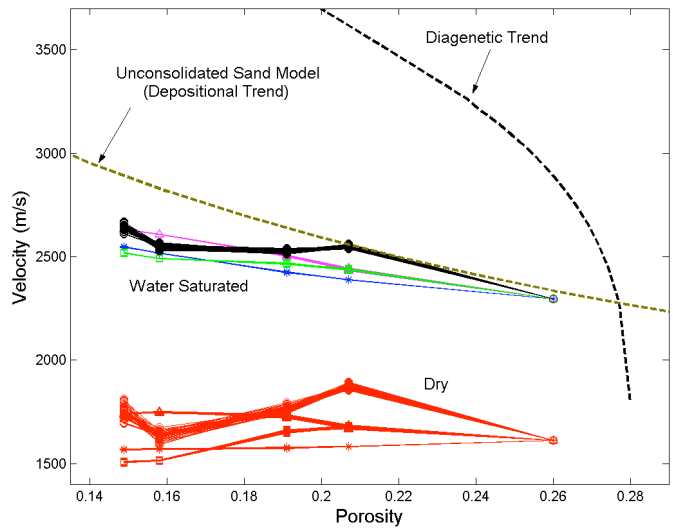

Figure B-14: Comparison of the results from the stochastic simulation with the rock-physics diagenetic trend and the unconsolidated sandstone model. The slope of the results, after fluid substitution, show a flatter trend than the one predicted from the unconsolidated sandstone model (modified Hashin-Strickman lower bound).

Comparison with Real Data

In essence, the theoretical modeling and the results from the stochastic simulations predict that the sorting effect has a flatter trend in the velocity-porosity plane than the packing effect. Whereas the MHSLB constitutes an upper bound to the sorting effect, it can be considered a lower bound for the packing effect. As shown below, both laboratory and subsurface data corroborate that the sorting effect follows a flatter trend than the MHSLB.

2.8.1. Comparison with Laboratory Data

There is good agreement between the sorting effect in both velocity and porosity observed in laboratory experiments (Zimmer, 2003), and the one predicted from the stochastic simulation (Figure B-15). The shown laboratory data correspond to measurements of sand and glass-bead aggregates with different sorting, at the same confining pressure (5 MPa). The samples were prepared under similar protocols; therefore, the porosity variation between samples is assumed to be exclusively caused by sorting (Zimmer, 2003). The lower porosity for the theoretical textural models is the consequence of the idealized rhombohedric packing, a very unlikely configuration for unconsolidated sands. The comparison, however, is based on the departure of each trend from its respective MHSLB. As can be observed in Figure B-15, the overall trend is

flatter than the MHSLB, especially because of the break in the trend as the sorting deteriorates. In the theoretical models, this break is driven by the introduction of the smaller spheres. A similar break is observed in the laboratory data, suggesting that indeed small spheres have a softening effect on the aggregate.

A better understanding of this comparison can be obtained by looking at the slope of the velocity change, rather than the actual velocity values (Figure B-16). In this comparison you can clearly see that the laboratory data show abrupt changes in the slope of the velocity-porosity trend. The MHSLB predicts a constantly increasing slope, which cannot reproduce the actual variability in the data. On the contrary, the results from the stochastic simulations reproduce the variable slopes, which overall create a flatter trend for the sorting effect.

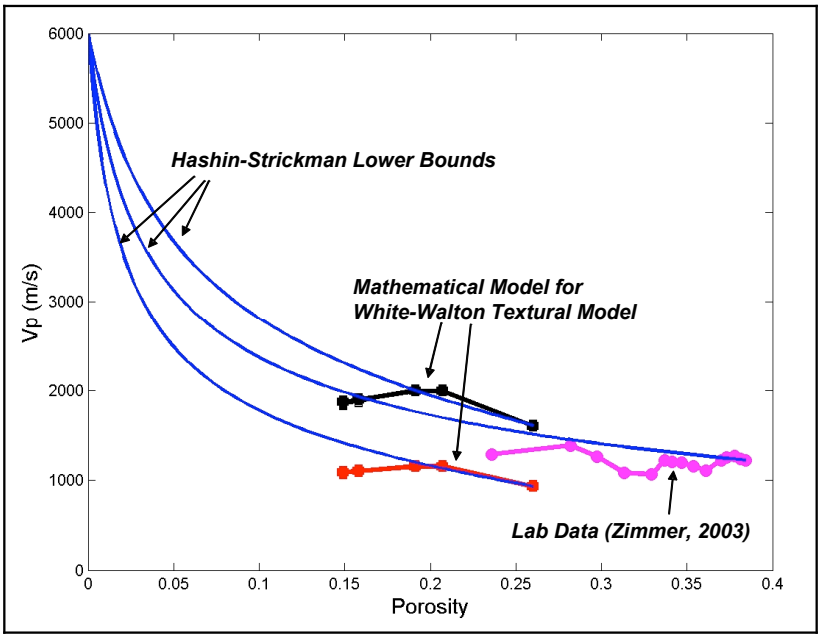

Figure B-15: Comparison of the theoretical results from stochastic simulation for water saturated (black) and dry (red) aggregates, and fluid-substituted laboratory measurements (magenta) performed by Zimmer (2003). Whereas the MHSLB predicts a gradually increasing velocity, both the results from the stochastic simulation and the laboratory data show a highly variable slope, which overall translates into a flatter trend for the sorting effect.

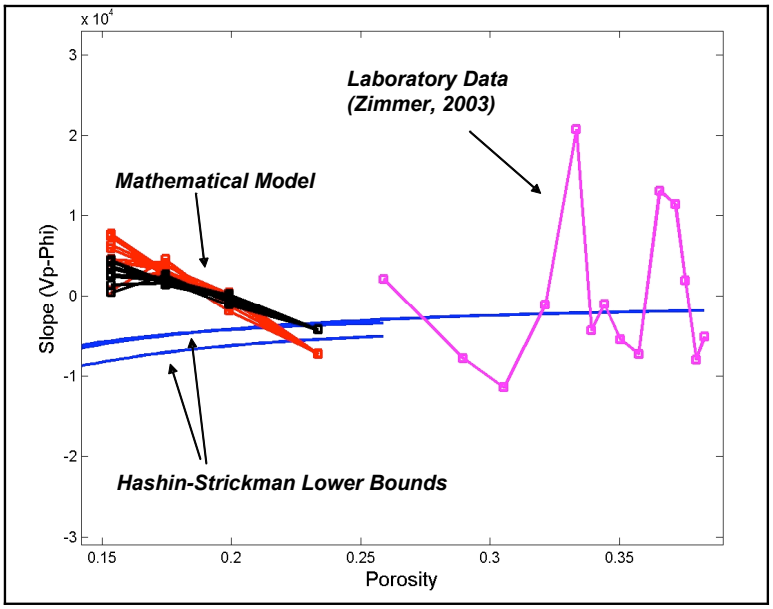

Figure B-16: Comparison of the velocity-porosity slopes predicted from MHSLB, the stochastic simulation, and the actual slopes observed in laboratory data. Contrary to MHSLB, the stochastic simulation based on the theoretical formulation presented here can generate variable slopes such as those observed in the data.

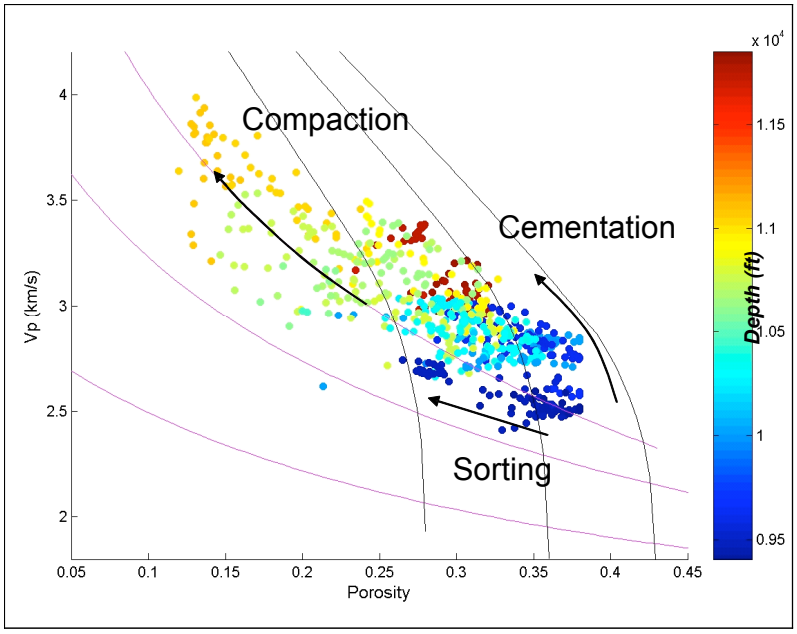

Figure B-17: Well-log data of sandstones from one single stratigraphic sequence within an oil field. The graph shows the three main trends for sandstones: the flat trend associated with the sorting effect, the compaction trend, and the steep diagenetic trend. As predicted from the theoretical model, the MHSLB constitutes an upper bound for the sorting trend.

2.8.2. Comparison with Subsurface Data

The velocity-porosity trend observed in uncemented sandstones in the subsurface agrees with the flat trend predicted from our theoretical analysis (Figure B-17). The flat trend is depicted by the shallower sands (blue dots in Figure B-17), and follows a gentler slope than the one predicted from the MHSLB (magenta lines in Figure B-17). The velocity and porosity data shown correspond to well-log measurements obtained along an interval where core porosity and sorting data were also available (Figure B-18 and Figure B-19). A least-squares regression was obtained for the correspondence between sorting and porosity from the core data (Figure B-19). The least-squares regression also indicates a small negative correlation between porosity and the grain size, which indicates a minor influence of packing, probably associated with grain angularity (fine grains tend to be more angular than coarser sands). However, the effect of sorting on porosity, in these sands, is stronger than the effect of packing. The high-porosity have better sorting than the low-porosity clean sands. These two different types of sands create the flat trend observed in the velocity-porosity plane.

The grain-size distribution was obtained from laser particle size analysis (LPSA). Similar data were available from other cores (Figure B-20), but the depth shifts required to compare with well-log data was not available. In both cases, the least-squares regressions show that although sorting has a strong effect on porosity, there is a small component associated with grain size itself (Figure B-21). This grain-size component is probably the effect of grain angularity, since finer grain sizes tend to be more angular. It is important to emphasize that the coefficient of variation (Sorting Index) of these log-normal distributions is the best parameter to model the relationship between sorting and porosity. Similarly, the median is a better measure of the average grain size than the mean. The combination of the two core data sets provide a linear regression that approximates the regressions obtained from previous laboratory data, and from the modeled quinary mixture (Figure B-5).

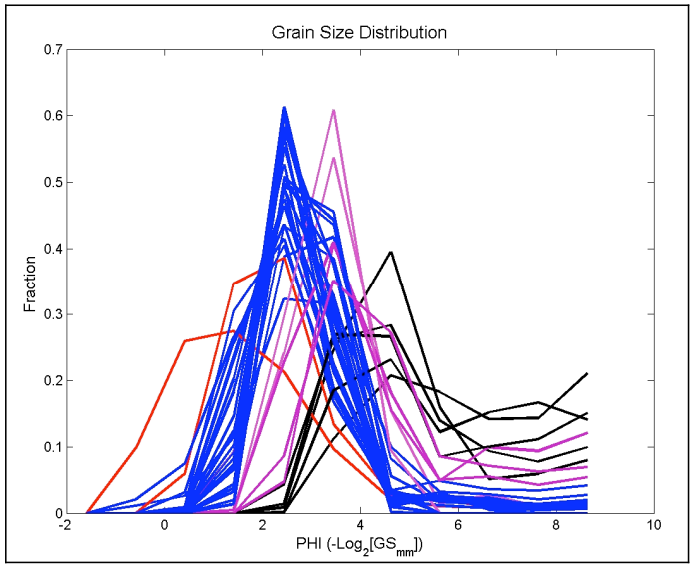

Figure B-18: LPSA grain-size distribution from core samples. The sampled interval corresponds to the same well-log data shown in Figure B-21.

$$\phi = -16.3883\left(\frac{\sigma}{\mu}\right) + 2.306\left(med_{PHI}\right) + 34.108$$

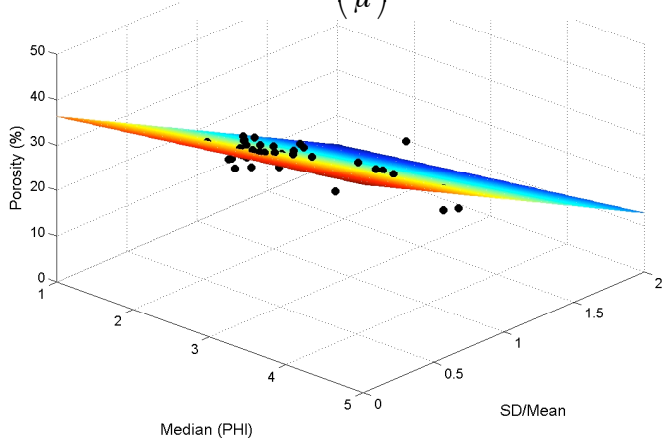

Figure B-19: Visualization of the least-squares regression between porosity (ϕ), the coefficient of variation (σ/μ), and the median grain size in PHI scale (med_{PHI}), from core samples. Porosity is given in percentage or porosity units. The samples are sandstones and correspond to the grain-size distributions shown in Figure B-18 and the well-log data shown in Figure B-19.

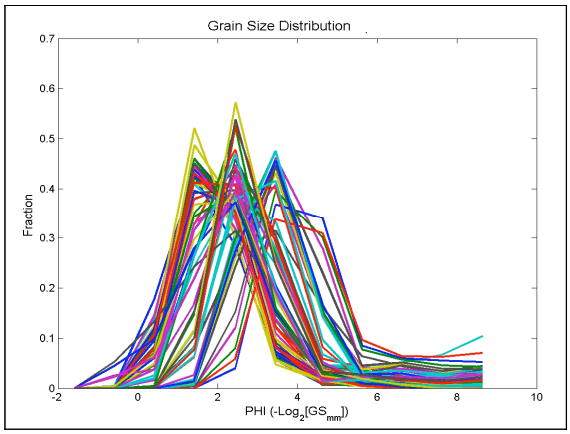

Figure B-20: LPSA grain-size distribution obtained from a different well and stratigraphic interval than the one shown in Figure B-18.

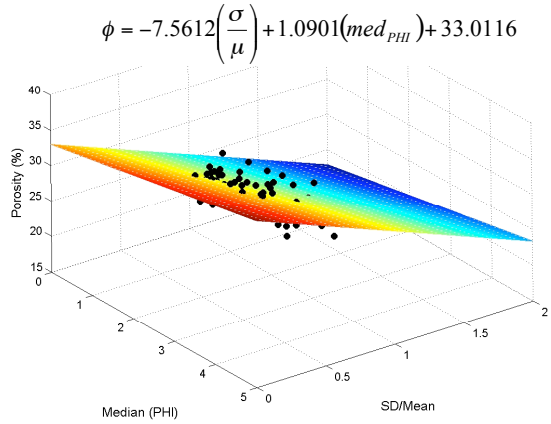

Figure B-21: Visualization of the least-squares regression between porosity, median grain size (PHI scale) and coefficient of variation, corresponding to the data shown in Figure B-20.

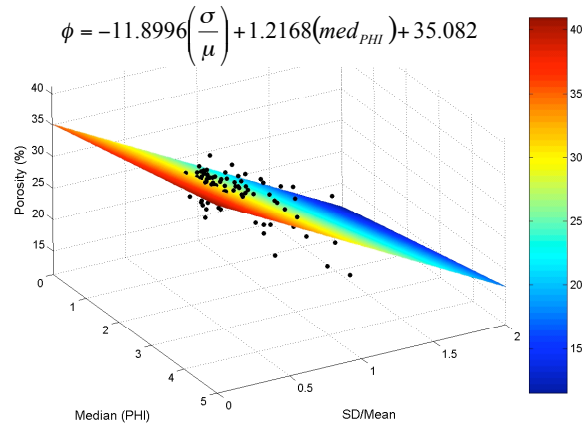

Figure B-22: Visualization of the least-squares regression between porosity, median grain size (PHI scale), and coefficient of variation, corresponding to the combination of the data shown in Figure B-18 and Figure B-20.

Discussion

Local and global average parameters and stochastic simulation have been necessary to introduce variable grain sizes into effective-medium contact models. A rigorous analytical solution of the elastic modulus of aggregates with variable grain size has not been the purpose of this work. Such a solution would vary depending on the spatial distribution of grain sizes. The stochastic approach followed in this work accounts for this variability, assuming is random, and allows us to evaluate the uncertainties associated with the local coordination number and the averaging methods. The results obtained by this approach suggest that statistical mechanics rather than deterministic solutions might be the right direction for further improvements in the effective-medium theory for granular aggregates.

The theoretical analysis, laboratory measurements, and subsurface data, all indicate that effect of sorting on the elastic properties of granular materials generates a flatter trend in the Vp-ϕ plane than the one predicted by the MHSLB. This flatter trend seems to be the consequence of a softening effect caused by introducing small spheres between large spheres. This softening effect of the small spheres is comparable to the effect of grain angularity analyzed by Bachrach *et al.* (2000). The effect has been theoretically modeled and observed in laboratory, and becomes evident in samples with large contrasts in grain size. For all practical purposes, the MHSLB should be considered an upper bound for the concomitant effect of sorting on the elastic properties and porosity of granular materials.

In contrast to the case of sorting, the MHSLB constitutes an approximate lower bound for the packing effect. The comparison of Hertz-Mindlin models, MHSLB and laboratory data shows that the trend associated with packing follows a steeper slope than the one predicted by any of these models. Grain stabilization and increasing grain-contact area by grain accommodation can both increase the aggregate stiffness. Zimmer (2003) obtained a similar conclusion. Bachrach (1998) modeled the variation in Poisson's ratio and shear stiffness based on the proportional increment of non-zero shear stiffness contacts. Since the slope predicted from both Hertz-Mindlin and the MHSLB models are similar, we can conclude that the MHSLB underestimates the actual packing trend.

Overall, the MHSLB constitutes a good approximation for the depositional trend in high-porosity sands (Avseth, 2000; Gutierrez and Dvorkin, 2001). The success of the MHSLB in reproducing the depositional trend might be the result of a combined effect of sorting and packing. Extension of the depositional trend to low-porosity sands should be cautiously done. The difference in surface area associated with changes in sorting may

influence the distribution of quartz cementation. Other factors like grain dissolution of feldspars may also have an effect. Although the trend observed in the velocity-porosity plane can be used to infer the variations in sorting of clean sands, it is always convenient to verify by looking at cuttings descriptions, thin sections and cores.

The effect of sorting on the elastic properties of high-porosity sands and sandstones differs from those of clay content and mechanical compaction. Although poor sorting is commonly associated with clay content, imposing an additional mineralogic effect on the elastic properties, the effect discussed here refers to grains with similar composition. For example, small amounts of clay can actually increase the elastic stiffness of an aggregate by acting as weak cementing material at the grain contacts (e.g. Dvorkin *et al.*, 1994). The sorting effect discussed here is independent and additional to the effect of clay content. On the other hand, mechanical compaction induces grain rearrangement, stabilization, and elastic deformation. Elastic deformation by itself does not induce a significant porosity reduction (e.g. Zimmer, 2003), and is induced by increasing confining stress. In contrast, grain rearrangement is an inelastic process that induces significant porosity reduction concomitant with the increment of the elastic stiffness. Grain rearrangement and stabilization tend to increase with depth, whereas sorting does not change with depth. Consequently, the gradual and concomitant variation of porosity and velocity with depth can be an additional criteria to distinguish between the sorting and packing effects.

Conclusions

The theoretical analysis presented in this paper indicates that the effect of sorting on both porosity and the elastic properties of granular materials differs from the effect of packing. This conclusion is also corroborated by the laboratory measurements and subsurface data. According to these results, variations in sorting generate a flatter trend in the velocity-porosity plane, with a slope gentler than the modified Hashin-Shtrikman lower bound (MHSLB). In contrast, variations in packing tend to generate a steeper slope than that predicted using the MHSLB. In general, whereas the MHSLB is a reasonable upper bound for the sorting effect, it constitutes a lower bound for the packing effect.

References

Allen, J. R. L., 2001, Principles of Physical Sedimentology, George Allen & Unwin (Publishers), London, 272 p.

Avseth, P., J. Dvorkin, G. Mavko, and J. Rykkje, 2000, Rock physics diagnostic of North Sea sands: Link between microstructure and seismic properties. Geophysical Research Letters, **27**, 2671-2764.

Avseth, P., 2000, Combining Rock Physics and Sedimentology for Seismic Reservoir Characterization in North Sea Turbidite Systems. Ph.D. thesis, Stanford University.

Bachrach, R., 1998, High-resolution shallow seismic subsurface characterization. Ph. D. thesis, Stanford University.

Bachrach, R., J. Dvorkin, and A. Nur, 2000, Seismic velocities and Poisson's ratio of shallow unconsolidated sands, Geophysics, **65**, 559-564.

Beard, D. C., and P. K. Weyl, 1973, Influence of texture on porosity and permeability of unconsolidated sand. American Association of Petroleum Geologists Bulletin, **15**, 2, 349-369.

Bourbie, T., O. Coussy, and B. Zinsner, 1987, Acoustics of Porous Media, Gulf Publishing Co., Houston, 334 pp.

Brandt, H., 1955, A study of the speed of sound in porous granular media, Journal of Applied Mechanics, **22**, 479-486.

Cumberland, D. J. and R. J. Crawford, 1987, The Packing of Particles, Elsevier Science Publishers, Amsterdam.

Digby, P. J., 1981, The effective elastic moduli of porous granular rocks, Journal of Applied Mechanics, **48**, 803-808.

Dvorkin, J., A. Nur, and H. Yin, 1994, Effective properties of cemented granular materials, Mechanics of Materials, 18, 351-366.

Dvorkin, J., and M. A. Gutierrez, 2001, Textural sorting effect on elastic velocities, part II: elasticity of a bimodal grain mixture, Society of Exploration Geophysicist Annual Meeting, Expanded Abstracts.

Estes, C.A., G. Mavko, H. H. Yin, and T. Cadoret, 1994, Measurements of velocity, porosity and permeability on unconsolidated granular materials, Stanford Rock Physics and Borehole Geophysics Project, annual report, **55**, G1-G9.

Fraser, H. J., 1935, Experimental study of the porosity and permeability of clastic sediments: Journal of Geology, **43**, 910-1010.

Fuchtbauer, H., 1974, Sediments and Sedimentary Rocks 1, in Sedimentary Petrology by W. v. Engelhardt, H. Fuchtbauer and G. Muller, Part II. John Wiley and Sons, New York, 464 pp.

Graton, L. C., and H. J. Fraser, 1935, Systematic packing of spheres –with particular relation to porosity and permeability: Journal of Geology, **43,** 785-909.

Gutierrez, M., 2001, Rock physics and 3D Seismic Characterization of Reservoir Heterogeneities to Improve Recovery Efficiency, Ph. D. dissertation, Stanford University.

Gutierrez, M., J. Dvorkin, and A. Nur, 2001, Textural sorting effect on elastic velocities, part I; laboratory observations, rocks physics models, and applications to field data, Society of Exploration Geophysicist Annual Meeting, Expanded Abstracts.

Inman, D. L., 1949, Sorting of sediments in the light of fluid mechanics, Journal of Sedimentary Petrology, **19**, 51-70.

Inman, D. L., 1956, Measures for describing the size distribution of sediments, Journal of Sedimentary Petrology, **22**, 125-145.

Johnson, K. L., 1985, Contact Mechanics, Cambridge University Press, 452 pp.

Kolbuszewski, J., 1948, An experimental study of the maximum and minimum porosities of sands, Proc. 2nd Int. Congress of Soil Mechanics, **7**, 47-49.

Krumblein, W. C., 1936, The use of quartile measures in describing and comparing sediments, American Journal of Science, **32**, 98-111.

Krumblein, W. C., 1938, Size frequency distributions of sediments and the normal phi curve, Journal of Sedimentary Petrology, **8**, 84-90.

Macrae, J. C. and W. A. Gray, 1961, Significance of the properties of materials in the packing of real spherical particles, Br. J. Appl. Phys., **12**, 162-172.

Marion, D., A. Nur, H. Yin, and D. Han, 1992, Compressional velocity and porosity in sand-clay mixtures, Geophysics, 57, 4, 554-563.

Mavko, G., J. Dvorkin, and T. Mukerji, 1998, The Rock Physics Handbook, tools for seismic analysis in porous media, Cambridge University press, New York, pp 329.

Mindlin, R. D., 1949, Compliance of elastic bodies in contact, Journal of Applied Mechanics, **16**, 259-268.

Murphy, D. W., III, 1982, Effect of Microstructure and Pore Fluids on The Acoustic Properties of Granular Sedimentary Materials, Ph. D. dissertation, Stanford University.

Nur, A., G. Mavko, J. Dvorkin, and D. Gal, 1995, Critical porosity: The key to relating physical properties to porosity I rocks, in Proc., 65th Annual International Meeting, Society of Exploration Geophysicists, 878.

Otto, G. H., 1939, A modified logarithmic probability graph for the interpretation of mechanical analyses of sediments, Journal of Sedimentary Petrology, **9**, 62-76.

Pettijohn, F. J., 1975, Sedimentary Rocks, 3rd edition, Harper and Row publishers, New York, 628 pp.

Rogers, J. J. and W. B. Head, 1961, Relationship between porosity, median size, and sorting coefficients of a synthetic sand, Journal of Sedimentary Petrology, **31**, 467-470.

Selley, R., 1988, Applied Sedimentology, Academic Press, San Diego, 523 pp.

Sohn, H. Y. and C. Moreland, 1968, The effect of particle size distribution on packing density, Canadian Journal of Chemical Engineering, **46**, 162-167.

Steinour, H. H., 1944, Rates of Sedimentation, Ind. Engng. Chem., **46**, 162-167.

Timoshenko, S. P., and J. N. Goodier, 1956, Theory of Elasticity, 2nd edition, McGraw-Hill, New York, 567 pp.

Trask, P. D., 1932, Origin and environments of source sediments of petroleum, Gulf Pub. Co., Houston, 323 pp.

Visher, G. S., 1969, Grain size distributions and depositional processes, Journal of Sedimentary Petrology, **39**, 1074-1106.

Visher, G. S., 1999, Stratigraphic Systems: Origin and Application, Academic Press, New York, 700 pp.

Walker, B. P., and T. Whitaker, 1967, An apparatus for forming uniform beds of sand for model foundations tests, Geotechnique, **17**, 161-167.

Walton, K., 1987, The effective elastic moduli of a random packing of spheres, Journ. Mech. Phys. Solids, **35**, 213-226.

Wentworth, C. K., 1922, A scale of grade and class terms for clastic sediments, Journal of Geology, **30**, 377-392.

White, H. E., and S. F. Walton, 1937, Particle packing and particle shape, Journal of the American Ceramists Society, **20**, 155-166.

Winkler, K. W., 1983, Contact stiffness in granular porous materials: comparison between theory and experiment, Geophysical Research Letters, **10**, 1073-1076.

Zimmer, M., M. Prasad, and G. Mavko, 2002, Empirical velocity-pressure and porosity-pressure trends in unconsolidated sands, SEG Annual Meeting, Expanded Technical Program Abstracts, **72**, 1866-1869.

Zimmer, M., 2003, Controls on the Seismic Velocities of Unconsolidated Sands: Measurements of Pressure, Porosity and Compaction Effects, Ph. D. dissertation, Stanford University.